Hindawi
International Journal of Aerospace Engineering
Volume 2021, Article ID 4490211, 19 pages
https://doi.org/10.1155/2021/4490211

Research Article

Three-Dimensional Prescribed-Time Pinning Group Cooperative Guidance Law

Wenhui Ma,[1] **Xiaogeng Liang**,[1,2] **Yangwang Fang**,[3] **Tianbo Deng**,[4] **and Wenxing Fu**[3]

[1]*School of Automation, Northwestern Polytechnical University, Xi'an 710072, China*
[2]*Luoyang Optoelectro Technology Development Center, Luoyang 471000, China*
[3]*Unmanned System Research Institute, Northwestern Polytechnical University, Xi'an 710072, China*
[4]*School of Astronautics, Northwestern Polytechnical University, Xi'an 710072, China*

Correspondence should be addressed to Wenxing Fu; wenxingfu@nwpu.edu.cn

Received 20 September 2021; Accepted 29 November 2021; Published 30 December 2021

Academic Editor: Chen Pengyun

In order to overcome the drawbacks of the convergence time boundary dependent on tuning parameters in existing finite/fixed-time cooperative guidance law, this paper presents a three-dimensional prescribed-time pinning group cooperative guidance scheme that ensures multiple unpowered missiles to intercept multiple stationary targets. Firstly, combining a prescribed-time scaling function with pinning group consensus theory, the prescribed-time consensus-based cooperative guidance law is proposed. Secondly, the prescribed-time convergence of the proposed pinning group consensus-based cooperative guidance law proves that the convergence can be achieved at a specified time, regardless of initial conditions and parameters. Furthermore, the design steps including two stages of the proposed guidance law are given for engineering application. Extensive simulations are carried out in three cases to verify the properties. Simulation results show the effectiveness and superiority of the proposed prescribed-time consensus-based cooperative guidance scheme.

1. Introduction

With the development of the advanced defense missile systems, such as the surface-to-air missile system and close-in weapon system, one-to-one has more obvious drawbacks in attacking or intercepting some equipped important tactical and strategic targets [1–3]. One of the effective countermeasures is cooperation. Obviously, the cooperative framework offers the major advantage that even if parts of missiles are neutralized by the defense system, the target interception will be achieved by the remaining missiles. Hence, the multimissile cooperative attack or interception problem is of great practical significance. To increase the lethality and probability of penetration, a lot of interest has been understandably paid to cooperative guidance in combat scenarios [4–15].

Compared with one-to-one engagement, cooperative engagement has advantages in effectively and comprehensively information detection or acquisition. As one of the initial efforts in this field, an impact time control guidance law (ITCG) is proposed for realizing salvo attack in [4]. To improve the precision strike, the consensus-based cooperative guidance scheme has arisen for increasing the penetration probabilities of multiple missiles. With the communication, the main objective of impact-time-related cooperation is achieving impact time consensus by adjusting relative distances and radial velocities to the target of each missile. Although existing powered missiles with controllable velocity shows better effectiveness in guidance accuracy [16–20], high cost is not conducive to giving full play to the advantages of scale. Therefore, coping with the unpowered multimissile cooperative guidance problem is more practical for engineering. Most of analytic results on unpowered cooperative guidance law considered the planar situations [21–25].

Note that most previous studies are dedicated for two-dimensional (2-D) unpowered cooperation engagements that ignore the couplings between the horizontal and vertical planners. Although 2-D guidance schemes can be applied in a realistic three-dimensional (3-D) scenario, its applications

need to be guaranteed by decoupling models. Generally, the pursuit situations are not confined only in one of the pitch and yaw planar planes but exist in the coupling between the motions. Nevertheless, aforementioned 3-D schemes are applicable to powered missiles, but they are limited by immature engine and high cost. Hence, the unpowered 3-D cooperative guidance is still an area to be studied. Since the 3-D guidance model was first introduced in [26], several researchers have concentrated on the studies of 3-D cooperative guidance law. With consensus theory, in [20, 27–30], auxiliary states were given to PPN-based cooperative guidance law for reducing the error of time-to-go estimation. With undirected graph, a distributed cooperative guidance law investigated in [27]. As to [28], an unpowered 3-D cooperative guidance law with constraint is proposed on the basis of undirected communication. However, the convergence conditions of aforementioned unpowered 3-D guidance law were established on the undirected topology. Though the consensus of the first-stage can be achieved, taking limited and power resources into consideration, uncertain convergence time may increase the negative influence of communication. Hence, proceeding from relaxing restrictions of communication with proper switch scheme is necessary for scale expansion.

As an effective solution, consensus-based cooperative guidance relies heavily on communication network. In essence, the network serves for the cooperation. The network framework of multimissile communication, which influences the quality and quantity of information, determines the topology directly. Due to the inherent importance of the communication network, consensus protocols for achieving the guidance cooperation have been widely researched for applications in different scenarios. Based on the proposed two-level hierarchical cooperative guidance architecture, Ref. [7] classified the cooperation into centralized and distributed. Furthermore, as a reliable way of centralized cooperation, the leader-follower scheme was utilized in multimissile cooperation widely [8–10]. Generally, the centralized structure has limitations such as not being conducive to the expansion of scale and strong dependence on network information. Therefore, more attention has turned to distributed cooperation with flexible communication. Derived from neighbour-to-neighbour communication, on the basis of a directed spanning tree, a distributed cooperative guidance law was designed in [11]. Although local neighbouring communication facilitates scale expansion, the incomplete information caused by network growth and distributed communication slows down the convergence rate. To keep the balance between astringency and expansibility, the integrated framework has earned more attention. In [31], under the directed topologies, an integrated cooperative framework with guidance layer, coordination layer, and control layer were proposed with formation containment tracking requirement. As to [32], an integrated framework provides a new solution for cooperatively against single stationary target by combining centralized and decentralized communication. For multiple centralized leader-follower groups, group communication is guaranteed by leaders, which means there is no communication between followers in a group.

In the aforementioned works, though different frameworks were utilized, only problems of multiple missiles against one single target were considered. However, important targets are usually shielded by defense systems. Hence, it is necessary to destroy the targets and their defense system together. In order to strike the multiple targets with cooperation, group consensus provides an effective way without time-to-go estimation [33–35]. To solve the unidirectional neighbour-to-neighbour communication limitation, a two-stage unpowered cooperative guidance law with directed group topology was first studied in [34]. On this basis, distributed group cooperative guidance law with switching directed communication topology was investigated. In [35], the study was further improved with directed communication and zero in-degree assumption. Thus, extensive researches are limited with conservative assumptions of the network so that unpowered group cooperative attack problems have not been studied extensively.

Considering the interception engagement, the convergence time is also an essential factor. Due to the limit of flight duration, the consensus of cooperation requires a faster convergence rate. To meet the demands of fast convergence, finite-time consensus-based cooperative guidance schemes show their superiorities. As presented in [22], the 2-D cooperative guidance law was designed via communication over a directed cycle graph, and consensus with time-to-go can be achieved at an apriority fixed finite time. With the small heading angle assumption, the 2-D time-go-to estimation has poor practicability for parts of scenarios. To ensure the fast convergence without estimation, in [20], a leader-follower cooperative guidance law was designed with a finite-time sliding mode method. Furthermore, to improve the effectiveness, the adaptive super-twisting sliding mode control with a new finite-time consensus protocol was developed in [36]. Although several efforts have been developed for finite-time cooperative guidance to achieve fast convergence, their effectiveness is affected by initial conditions. Recently, research has turned to the fixed-time theory's application in cooperative guidance [37–39]. Independent of initial conditions, practicability of fixed-time cooperative guidance law was enhanced. However, the bound of settling time in these fixed-time consensus algorithms was calculated via the conservation, which means that the upper bound of the settling time is still related to system parameters, and usually, its estimated value is larger than the real settling time. Therefore, the convergence time of existing fixed-time cooperative guidance is unable to be prescribed. Though there have been several studies on prescribed-time consensus [40, 41], study on 3-D prescribed-time unpowered cooperative guidance has not been studied extensively. According to these observations, for cooperative interception, the prescribed-time consensus-based cooperative guidance law can provide better convergent conditions for the latter flight mission. Therefore, exploring the prescribed-time consensus-based cooperative guidance law is meaningful.

Motivated by the above discussions, this paper attempts to design a novel 3-D two-stage prescribed-time

pinning group cooperative guidance law for more general topology. The main benefits are summarized as the following aspects.

(1) Different from the existing finite/fixed-time cooperative guidance law, independent of retuning parameters or initial conditions, the proposed cooperative guidance law can ensure prescribed-time convergence according to the mission

(2) The second-order prescribed-time pinning group framework is proposed for improving the coordination. Utilizing the pinning group consensus, the prescribed-time group guidance framework is improved with the pinning scheme. Compared with other existing works in [33–35] with zero in-degree balance assumption, the convergence condition is relaxed by a pinning-based M-matrix and the convergence time can be specified. Obviously, a network with a topology that allows for interactions from other subgroups is more practical

(3) The 3-D two-stage prescribed-time cooperative guidance scheme is provided for practical applications. By using the proposed prescribed-time consensus-based cooperative guidance law in the first stage, the convergence can be realized at a desirable switching time. On this basis, the individual PPN guidance law in the second phase significantly reduces the cost of the network integration. Hence, with the 3-D two-stage prescribed-time cooperative scheme based on the simplified pinning group framework, unpowered missiles' cooperation is beneficial for reducing cost in practice.

The remainder of this study is organized as follows. In Section 2, preliminaries and problem formulation are presented. The main results of three-dimensional two-stage prescribed-time pinning group cooperative guidance scheme is provided in Section 3. Considering different scenarios, Section 4 provides numerical simulation results for verification. Section 5 concludes the whole work.

2. Preliminaries and Problem Statement

In this section, the research background and some necessary preliminaries are discussed in detail. Firstly, the three-dimensional homing engagement geometry of a missile in one group against its target is established. On this basis, the pure proportional navigation guidance law is given. Then, in order to describe the communication network of the multiple missiles, some concepts and lemmas of M -matrix and prescribed-time convergence are introduced. To achieve the cooperative missions, the control objective is presented with some assumptions.

2.1. Basic Assumptions. For simplification, the relative kinematics of the multiple missiles and targets are established on the basis of the following assumptions: (1) In the three-dimensional space, all the missiles are considered as mass points in the three dimensional. (2) All missiles are unpowered with the same constant speed. The acceleration is perpendicular to its velocity. (3) The seekers' and autopilots' dynamics are fast enough in comparison with the guidance loop.

2.2. Formulation of the Three-Dimensional PPN Guidance Law. To describe the cooperative engagement geometry, the relative motion relationship of the i-th missile belonging to the g_i-th subgroup attacking task-specified target T_γ is shown in Figure 1, where *LOS* is the abbreviated form of line-of-sight, $M_i - X_I Y_I Z_I$ is the reference coordinate system, and $M_i - X_{M_i} Y_{M_i} Z_{M_i}$ is the missile body coordinate system. r_i denotes the range between the i-th missile and target, and V_M represents the velocity vector. As for θ_{mi} and ψ_{mi}, they are two Euler angles for the *LOS* coordinate system to the body coordinate system of M_i. θ_{Li} and ψ_{Li} represent *LOS* angles in the azimuth and elevation directions, respectively. Following this, the 3-dimensional geometry is established on the basis of the point-mass assumption. Referring to Ref. [1], the engagement kinematic is outlined as

$$\begin{cases} \dot{r}_i = -V_M \cos\theta_{mi} \cos\psi_{mi}, \\ r_i \dot{\lambda}_{yi} = V_M \sin\theta_{mi}, \\ r_i \dot{\lambda}_{zi} = -V_M \cos\theta_m \sin\psi_m, \\ \dot{\theta}_{mi} = \dfrac{A_{zmi}}{V_m} - \dfrac{V_M}{r_i} \tan\lambda_{yi} \cos\theta_{m_i} \sin^2\psi_{mi} + \dfrac{V_M}{r_i} \sin\theta_{mi} \cos\psi_{mi}, \\ \dot{\psi}_{mi} = \dfrac{A_{ymi}}{V_m \cos\theta_{mi}} + \dfrac{V_M}{r_i} \tan\lambda_{yi} \sin\theta_{mi} \sin\psi_{mi} \cos\psi_{mi} \\ + \dfrac{V_M}{r_i \cos\theta_{mi}} \sin^2\theta_{mi} \sin\psi_{mi} + \dfrac{V_M}{r_i} \cos\theta_{mi} \sin\psi_{mi}, \end{cases} \tag{1}$$

where λ_{yi} and λ_{zi} are *LOS* angle components in the inertial reference frame and A_{ymi} and A_{zmi} are normal accelerations of M_i in the yaw and pitch directions, respectively. Subsequently, the heading error σ_i, which represents the field-of-view of the missile's seeker, is defined with Euler angles as

$$\sigma_i = \arccos\left(\cos\theta_{mi} \cos\psi_{mi}\right), \quad \sigma_i \in [0, \pi). \tag{2}$$

Hence, the 3-dimensional PPNG law is given as

$$\begin{cases} A_{ymi\_PPN} = -KV_M \dot{\lambda}_{yi} \sin\theta_{mi} \sin\psi_{mi} + KV_M \dot{\lambda}_{zi} \cos\theta_{mi}, \\ A_{zmi\_PPN} = -KV_M \dot{\lambda}_{yi} \cos\psi_{mi}, \end{cases} \tag{3}$$

where K is the navigation gain of the PPN which guarantees the convergence of the heading error during the terminal guidance.

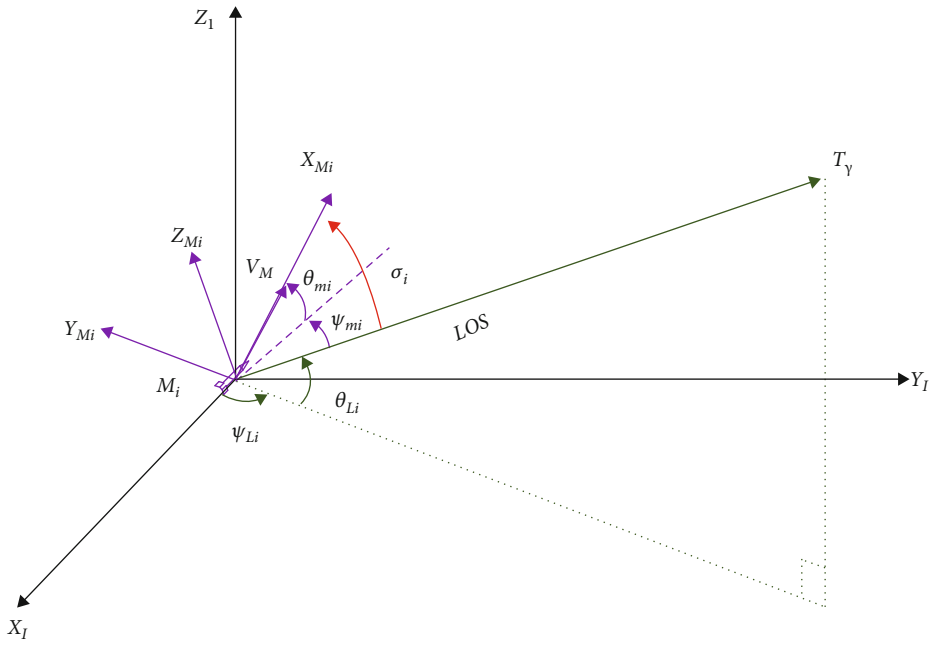

Figure 1: Geometry of missile and target in 3-dimensional.

Differentiating Equation (2) with respect to time t and substituting Equation (3) into it yields

$$\begin{aligned}\dot{\sigma}_i &= \frac{1}{\sin\sigma_i}\left(\sin\theta_{mi}\cos\psi_{mi}\dot{\theta}_{mi} + \cos\theta_{mi}\sin\psi_{mi}\dot{\psi}_{mi}\right)\\ &= -\frac{(K-1)}{\sin\sigma_i}\frac{V_M}{r_i}\left(\cos^2\psi_{mi} - \cos^2\theta_{mi}\cos^2\psi_{mi} + \sin^2\psi_{mi}\right)\\ &= -\frac{(K-1)V_M}{r_i}\sin\sigma_i.\end{aligned} \tag{4}$$

Subsequently, the following expression is obtained:

$$\frac{\partial r_i}{\partial\sigma_i} = \frac{r_i\cot\sigma_i}{K-1}. \tag{5}$$

Solving Equation (5), the range-to-go can be obtained as

$$r_i = \frac{r_i(0)}{|\sin\sigma_i(0)|^{1/(K-1)}}|\sin\sigma_i|^{1/(K-1)}, \tag{6}$$

which implies that missiles guided by the typical PPN exhibit the same flight trajectory with the same initial conditions of the range-to-go and heading error. This valuable information plays an important role in the following section in designing the cooperative guidance scheme for different scenarios.

Substituting Equation (6) into (4), we can obtain that

$$\dot{\sigma}_i = -\frac{(K-1)V_M|\sin\sigma_i(0)|^{1/(K-1)}}{r_i(0)}|\sin\sigma_i|^{(K-2)/(K-1)}, \tag{7}$$

which indicates that convergence of the heading error will be guaranteed with the navigation gain $K \geq 2$.

Remark 1. For the size of stationary targets in nonzero, when a cooperative attack of interception happens, r_i belongs to the interval $r_s \in [r_{\text{smax}}, r_{\text{smin}}]$. Hence, the following inequality holds during the entire flight:

$$r_s \leq r_i(t) \leq \max\left(r_i(0)\right), \tag{8}$$

where $\max\left(r_i(0)\right)$ denotes the maximum initial range-to-go of the i-th missile.

2.3. Preliminaries. In this paper, the homogeneous cooperation group containing N missiles are divided into $\kappa(\kappa \geq 2)$ subgroups for attacking. For the multimissiles' cooperation, communication network between missile nodes and subgroups is essential. Herein, the directed graph $G = (\mathscr{H}, \mathscr{E}, A)$ is utilized to describe the communication network, where $\mathscr{H} = \{v_i, \cdots, v_N\}$ denotes the N-missile set and $\mathscr{E} = \{(i,j) \in \mathscr{H} \times \mathscr{H}\}$ represents the relationship between missiles in the topology, in which $(v_i, v_j) \in \mathfrak{E}$ represents the j-th missile which can receive information from the i-th missile. The weight adjacency matrix is defined as $A = \{a_{ij}\}$, where $a_{ii} = 0$, $a_{ij} > 0$ if and only if $(v_i, v_j) \in \mathfrak{E}$, otherwise $a_{ij} = 0$. Accordingly, the Laplacian matrix $\mathscr{L} = \{l_{ij}\}$ associated with A is defined as

$$l_{ij} = \begin{cases} \sum_{j=1, j\neq i}^{N} a_{ij}, & j = i,\\ -a_{ij}, & j \neq i,\end{cases} \tag{9}$$

which guarantees that $\sum_{j=1}^{N} l_{ij} = 0$, $i = 1, 2, \cdots, N$.

Subsequently, some lemmas are given for derivation.

Definition 2. A nonsingular matrix $A = \{a_{ij}\} \in R^{N\times N}$ is defined as a M-matrix if all the elements satisfy $a_{ij} \le 0 (i \ne j)$ and all the elements of A^{-1} are nonnegative.

Definition 3. A diagonal matrix $A = \text{diag}\{a_i\} \in R^{N\times N}$ is defined as a pinning matrix, if diagonal elements $a_i = 1$ mean that the i-th node is pinned, otherwise $a_i = 0$.

Lemma 4 (see [42]). *For a nonsingular matrix $A = \{a_{ij}\} \in R^{N\times N}$, the following statements are equivalent: (1) A is a M-matrix; (2) all eigenvalues of A have a positive real part, which means $\text{Re}(\lambda_i(A)) > 0, i = 1, 2, \cdots, N$; (3) there exists a positive definite diagonal matrix $\Xi = \text{diag}[\xi_1, \xi_2, \cdots, \xi_N] > 0$, such that $\Xi A + A^T \Xi$ is positive definite.*

Lemma 5 (see [40]). *For any given vectors A and B, if there is any arbitrarily positive definite matrix W, the following inequality holds:*

$$2A^T B \le A^T W A + B^T W^{-1} B. \tag{10}$$

A time-varying function for the specified time convergence is defined as the following form:

$$\zeta(t) = \begin{cases} \left(\dfrac{T}{t_0 + T - t}\right)^h, & t \in [t_0, t_0 + T), \\ 1, & t \in [t_0 + T, \infty), \end{cases} \tag{11}$$

where $h > 1$, t_0 is the start time, and T is the user's assigned convergence time.

The time derivative of Equation (11) can be expressed as

$$\dot{\zeta}(t) = \begin{cases} \dfrac{h}{T}\left(\dfrac{T}{t_0 + T - t}\right)^{h+1}, & t \in [t_0, t_0 + T), \\ 0, & t \in [t_0 + T, \infty). \end{cases} \tag{12}$$

Lemma 6 (see [41]). *Considering a dynamic system described by $\dot{x} = f(t, x(t)), x(0) = x_0$, where $x \in R^N$ and $f(\bullet, \bullet)$ is a function bounded in time. There exists a continuously differentiable function $V(t, x(t))$ denoted as $V(t)$ in short with $V(t, 0) = 0$. If there exists $\dot{V}(t) \le -\eta V(t) - \mu(\dot{\zeta}(t)/\zeta(t))V(t)$ with constants $\eta \ge 0$ and $\mu > 0$, then the system is globally prescribed-time stable. Moreover, for $t \in [t_0, t_0 + T)$, it satisfies $\dot{V}(t) \le \zeta^{-\mu(t)} e^{-\eta(t-t_0)} V(t_0)$, and for $t \in [t_0 + T, \infty)$, it holds that $V(t) \equiv 0$.*

3. Main Results

In this section, a novel 3-D prescribed-time cooperative guidance law is designed. Then, the two-stage cooperative guidance scheme is given for practical implementation. Finally, a design flow is introduced for real application.

3.1. Design of Prescribed-Time Cooperative Guidance Law. Suppose that impact time t_f is the total time taken by the missile from predefined reference terminal guidance starting time to the moment of hitting its target. As to time-to-go, it is defined as the total time remaining till the missile hitting its target. So, we have $t_f = t_{go} + t$. Traditionally, the estimation method of the time-to-go is established on the small heading error assumption. However, the heading error not only influences on the estimation of the time-to-go but also represents the movement of the seeker. The smaller the heading angle is, the closer the target is to the center of the field-of-view, which benefits the target capture and impact-time cooperation. Hence, the state variables are selected as

$$x_{1i} = \frac{r_i}{V_M} + t, x_{2i} = -\cos\sigma_i + 1, \quad i = 1, 2, \cdots, N. \tag{13}$$

Remark 7. r_i and σ_i can be measured by radar or inertial measurement unit in practical engineering. When $\sigma_i = 0$, x_{1i} represents the arrival time. However, for the existence of heading error, x_{1i} can be used as an auxiliary state rather than the approximated arrival time. In addition, heading error represents the position of the target in the field-of-view. The smaller heading angle benefits targeting. Hence, the state variable setting is similar in terms of the control objective, which is used for cooperatively generating the desired range-to-go without the heading angle.

Accordingly, time derivatives of state variables can be calculated as

$$\begin{cases} \dot{x}_{1i} = x_{2i}, \\ \dot{x}_{2i} = \dfrac{A_{zmi\_co}}{V_M}\sin\theta_{mi}\cos\psi_{mi} + \dfrac{A_{ymi\_co}}{V_M}\sin\psi_{mi} \\ + \dfrac{V_M}{r_i}\sin^2\theta_{mi} + \dfrac{V_M}{r_i}\cos^2\theta_{mi}\sin^2\psi_{mi}. \end{cases} \tag{14}$$

The N-missile group containing κ subgroups denote as $\boldsymbol{g} = \boldsymbol{g}_1 \cup \boldsymbol{g}_2 \cup \cdots \boldsymbol{g}_{g_i} \cup \cdots \cup \boldsymbol{g}_\kappa$, where the i-th missile belongs to the g_i-th group and its group's assigned state variable is represented with subscript g_i, such as the heading angle σ_{g_i}. The design objective of the cooperative guidance law can be expressed as prescribed-time cooperative attack in Definition 8.

Definition 8. The multimissile system Equation (14) is said to be group prescribed-time cooperative attack if

$$\begin{cases} \lim\limits_{t\to t_0+T} |r_i(t) - r_j(t)| = 0, \quad i, j \in \boldsymbol{g}_{g_i}, \\ \lim\limits_{t\to t_0+T} |\sigma_i(t) - \sigma_j(t)| = 0 \text{ or } \lim\limits_{t\to t_0+T} |\cos\sigma_i(t) - \cos\sigma_j(t)| = 0, \quad i, j \in \boldsymbol{g}_{g_i}, \\ \lim\limits_{t\to t_0+T} |r_{f,i}(t) - r_{f,g_i}(t)| = 0, \quad i \in \boldsymbol{g}, \\ \lim\limits_{t\to t_0+T} |\sigma_i(t) - \sigma_{g_i}(t)| = 0 \text{ or } \lim\limits_{t\to t_0+T} |\cos\sigma_i(t) - \cos\sigma_{g_i}(t)| = 0, \quad i \in \boldsymbol{g}, \end{cases} \tag{15}$$

and for $\forall t \geq t_0 + T$,

$$\begin{cases} \left|r_i(t) - r_j(t)\right| = 0, & i, j \in \mathcal{G}_{g_i}, \\ \left|r_{f,i}(t) - r_{f,g_i}(t)\right| = 0, & i \in \mathcal{G}, \\ \left|\sigma_i(t) - \sigma_{g_i}(t)\right| = 0 \text{ or } \left|\cos\sigma_i(t) - \cos\sigma_{g_i}(t)\right| = 0, & i \in \mathcal{G}. \end{cases} \tag{16}$$

Assumption 9. $\mathcal{L} + D$ is a M-matrix, where $\mathcal{L}$ is a Laplacian matrix of a group topology and D is a pinning matrix.

Assumption 10. There exist parameters $h > 1$, $T > 0$, $\iota_1 > 0$, $\iota_2 > 0$, $\beta_2 > 0$, $\beta_0 > \beta_1^2/\beta_2 h\varpi_2$ and $\eta \geq 0$, such that

$$\frac{2}{h} < \mu < -\frac{T}{h}\left(\eta + \max\left(\frac{\Omega_1}{\Omega_2}, \frac{\Omega_3}{\Omega_4}\right)\right), \tag{17}$$

where

$$\begin{cases} \Omega_1 = \dfrac{h}{T}\left[\left(\beta_0 - \alpha_1\beta_1 + \dfrac{h\beta_0 + \alpha_1\beta_2}{4\iota_1}\right)\varpi_2 + \beta_1\left(\dfrac{1}{h} + \alpha_2\right)\dfrac{1}{4\iota_2}\right] < 0, \\ \Omega_2 = \varpi_1 h\beta_0 + \dfrac{\beta_1}{2\iota_2}, \\ \Omega_3 = \dfrac{h}{T}\left[\beta_1 - \alpha_2\beta_2 + \beta_1\left(\dfrac{1}{h} + \alpha_2\right)\iota_2 + (h\beta_0 + \alpha_1\beta_2)\iota_1\varpi_1\right] < 0, \\ \Omega_4 = (\beta_2 + 2\beta_1\iota_2), \end{cases} \tag{18}$$

where α_1 and α_2 are guidance gains and η and μ are parameters defined in Lemma 4; Ξ defined in Lemma 6 satisfies $\Gamma = \Xi(\mathcal{L} + D) + (\mathcal{L} + D)^T\Xi$ with $\varpi_1 = \lambda_{\max}(\Gamma)/\lambda_{\min}(\Xi)$ and $\varpi_2 = \lambda_{\min}(\Gamma)/\lambda_{\max}(\Xi)$.

Accordingly, the following theorem for the proposed prescribed-time cooperative guidance law is given.

Theorem 11. *Suppose Assumptions 9 and 10 are satisfied. If there exists the group prescribed-time cooperative guidance law Equation (19), the multimissile system Equation (14) can achieve the group prescribed-time cooperative attack at prescribed-time $t_0 + T$.*

$$\begin{cases} A_{ymi\_co} = -\dfrac{V_M^2}{r_i}\sin\psi_{mi} + \dfrac{U_i V_M}{2\sin\psi_{Mi}}, \\ A_{zmi\_co} = -\dfrac{V_M^2}{r_i}\sin\theta_{mi}\cos\psi_{mi} + \dfrac{U_i V_M}{2\sin\theta_{Mi}\cos\psi_{Mi}}, \end{cases} \tag{19}$$

where $U_i = -\alpha_2(\dot\zeta(t)/\zeta(t))(x_{2i}(t) - x_{2,g_i}) + \alpha_1(\dot\zeta(t)/\zeta(t))^2 \sum_{j\neq i, j=1}^N a_{ij}(x_{1j}(t) - x_{1i}(t)) + \alpha_1(\dot\zeta(t)/\zeta(t))^2\sum_{j=1}^N l_{ij}x_{1,g_j} + p_i$ *with pinning command* $p_i = -\alpha_1 d_i(\dot\zeta(t)/\zeta(t))^2(x_{1i}(t) - x_{1,g_i})$, $i, j \in \mathcal{G}$.

Proof. The proof of prescribed-time convergence will be divided into three parts. We first prove that pinning group consensus can be achieved in the assigned time T. Then, the consensus is kept over $[t_0 + T, \infty)$ with input remaining zero is proven. Finally, the proof that the control input keeping C^0 smooth over $[t_0, \infty)$ is given.

(i) Pinning group consensus in specified time T

In order to prove pinning group consensus by Lyapunov stability theorem, we first proceed several system transformations.

Substituting Equation (19) into Equation (14), the multimissile system can be described by a double-integrator system

$$\begin{cases} \dot x_{1i} = x_{2i}, \\ \dot x_{2i} = U_i, \end{cases} \tag{20}$$

where U_i is regarded as a control input. By introducing the pinning scheme, the prescribed-time group consensus with general coupling topology is extended and complemented by the group consensus results in [42] from single-order to second-order system with prescribed-time scaling function. In view of Equation (19), the pinning group controller can be rewritten as

$$\begin{aligned} U_i &= -\alpha_2\frac{\dot\zeta(t)}{\zeta(t)}\left(x_{2i}(t) - x_{2,g_i}\right) - \alpha_1 d_i\left(\frac{\dot\zeta(t)}{\zeta(t)}\right)^2\left(\left(x_{1i}(t) - x_{1,g_i}\right)\right. \\ &\quad + \alpha_1\left(\frac{\dot\zeta(t)}{\zeta(t)}\right)^2 l_{ii}x_{1,g_i} + \alpha_1\left(\frac{\dot\zeta(t)}{\zeta(t)}\right)^2\sum_{j\neq i, j=1}^N a_{ij}(x_{1j}(t) - x_{1i}(t)) \\ &\quad - \alpha_1\left(\frac{\dot\zeta(t)}{\zeta(t)}\right)^2\sum_{j\neq i, j=1}^N a_{ij}x_{1,g_j} = -\alpha_2\frac{\dot\zeta(t)}{\zeta(t)}\left(x_{2i}(t) - x_{2,g_i}\right) \\ &\quad - \alpha_1 d_i\left(\frac{\dot\zeta(t)}{\zeta(t)}\right)^2\left(\left(x_{1i}(t) - x_{1,g_i}\right) + \alpha_1\left(\frac{\dot\zeta(t)}{\zeta(t)}\right)^2\sum_{j\neq i, j=1}^N a_{ij}x_{1,g_i}\right. \\ &\quad + \alpha_1\left(\frac{\dot\zeta(t)}{\zeta(t)}\right)^2\sum_{j\neq i, j=1}^N a_{ij}(x_{1j}(t) - x_{1i}(t)) - \alpha_1\left(\frac{\dot\zeta(t)}{\zeta(t)}\right)^2\sum_{j\neq i, j=1}^N a_{ij}x_{1,g_j} \\ &= -\alpha_2\frac{\dot\zeta(t)}{\zeta(t)}\left(x_{2i}(t) - x_{2,g_i}\right) - \alpha_1 d_i\left(\frac{\dot\zeta(t)}{\zeta(t)}\right)^2\left(x_{1i}(t) - x_{1,g_i}\right) \\ &\quad + \alpha_1\left(\frac{\dot\zeta(t)}{\zeta(t)}\right)^2\sum_{j\neq i, j=1}^N a_{ij}\left(\left(x_{1j}(t) - x_{1,g_j}\right) - \left(x_{1i}(t) - x_{1,g_i}\right)\right) \\ &= -\alpha_2\frac{\dot\zeta(t)}{\zeta(t)}\left(x_{2i}(t) - x_{2,g_i}\right) - \alpha_1\left(d_i + \sum_{j=1}^N l_{ij}\right)\left(\frac{\dot\zeta(t)}{\zeta(t)}\right)^2\left(\left(x_{1i}(t) - x_{1,g_i}\right)\right). \end{aligned} \tag{21}$$

Let $E_1 = X_1(t) - X_{1,\mathcal{G}}$ and $E_2 = X_2(t) - X_{2,\mathcal{G}}$; it can be obtained that

$$U = -\alpha_2\frac{\dot\zeta(t)}{\zeta(t)}\mathrm{E}_2 - \alpha_1\left(\frac{\dot\zeta(t)}{\zeta(t)}\right)^2(\mathcal{L} + D)\mathrm{E}_1, \tag{22}$$

where $U = [U_1, U_2, \cdots, U_N]^T \in R^{1\times N}$, $X_1 = [x_{11}, x_{12}, \cdots, x_{1N}]^T \in R^{1\times N}$, $X_2 = [x_{21}, x_{22}, \cdots, x_{2N}]^T \in R^{1\times N}$, $X_{1,\mathcal{G}} =$

$[x_{1,g_1}, x_{1,g_2}, \cdots, x_{1,g_N}]^T \in R^{1\times N}$, $X_{2,\mathscr{g}} = [x_{2,g_1}, x_{2,g_2}, \cdots, x_{2,g_N}]^T \in R^{1\times N}$.

Let $\widehat{E}_1 = (\dot{\zeta}(t)/\zeta(t))E_1, \widehat{E}_2 = E_2$; the system (20) can be transformed as follows:

$$\begin{cases} \dot{\widehat{E}}_1(t) = \dfrac{\dot{\zeta}(t)}{\zeta(t)}\widehat{E}_2(t) + \dfrac{\dot{\zeta}(t)}{h\zeta(t)}\widehat{E}_1(t), \\ \dot{\widehat{E}}_2(t) = -\alpha_2\dfrac{\dot{\zeta}(t)}{\zeta(t)}\widehat{E}_2 - \alpha_1\dfrac{\dot{\zeta}(t)}{\zeta(t)}(\mathscr{L}+D)\widehat{E}_1. \end{cases} \tag{23}$$

Hence, denote

$$H = \begin{bmatrix} \dfrac{1}{h}I_N & I_N \\ -\alpha_1(\mathscr{L}+D) & -\alpha_2 I_N \end{bmatrix}. \tag{24}$$

System (23) can be rewritten as

$$\dot{\widehat{E}} = \frac{\dot{\zeta}(t)}{\zeta(t)}H\widehat{E}, \tag{25}$$

where $\widehat{E} = [\widehat{E}_1, \widehat{E}_2] \in R^{1\times 2N}$.

In the following, we can prove the pinning group consensus in specified time T based on Equation (25). A candidate Lyapunov function is set as

$$V = \frac{1}{2}E\wedge^T\Psi\widehat{E}, \tag{26}$$

where

$$\Psi = \begin{bmatrix} \beta_0 h\Gamma & \beta_1\Xi \\ \beta_1\Xi & \beta_2\Xi \end{bmatrix}. \tag{27}$$

According to Schur's Complement Lemma, when $\beta_0 > 0$ and $\beta_0 h\Gamma - \beta_1\Xi(\beta_2\Xi)^{-1}\beta_1\Xi$, then $\Psi > 0$. Hence, if $\beta_2 > 0$ and $\beta_0 > \beta_1^2/\beta_2 h\varpi_2$ hold, then $V > 0$.

Calculating the time derivative of V along Equation (14) and substituting Equation (22) into it gives

$$\dot{V} = \frac{\dot{\zeta}(t)}{\zeta(t)}\Big[(\beta_0-\alpha_1\beta_1)\widehat{E}_1^T\Gamma\widehat{E}_1 + (\beta_1-\alpha_2\beta_2)\widehat{E}_2^T\Xi\widehat{E}_2 + \beta_0 h\widehat{E}_1^T\Gamma\widehat{E}_2 - \alpha_2\beta_1\widehat{E}_1^T\Xi\widehat{E}_2 + \frac{\beta_1}{h}\widehat{E}_2^T\Xi\widehat{E}_1 - \alpha_1\beta_2\widehat{E}_2^T\Xi(L+D)\widehat{E}_1\Big]. \tag{28}$$

According to Lemma 5, the cross terms satisfy

$$\begin{cases} \pm\widehat{E}_1^T\Gamma\widehat{E}_2 \le \dfrac{1}{4\iota_1}\widehat{E}_1^T\Gamma\widehat{E}_1 + \iota_1\widehat{E}_2^T\Gamma\widehat{E}_2 \text{ or } \pm\widehat{E}_2^T\Gamma\widehat{E}_1 \le \dfrac{1}{4\iota_1}\widehat{E}_1^T\Gamma\widehat{E}_1 + \iota_1\widehat{E}_2^T\Gamma\widehat{E}_2, \\ \pm\widehat{E}_1^T\Xi\widehat{E}_2 \le \dfrac{1}{4\iota_2}\widehat{E}_1^T\Xi\widehat{E}_1 + \iota_2\widehat{E}_2^T\Xi\widehat{E}_2 \text{ or } \pm\widehat{E}_2^T\Xi\widehat{E}_1 \le \dfrac{1}{4\iota_2}\widehat{E}_1^T\Xi\widehat{E}_1 + \iota_2\widehat{E}_2^T\Xi\widehat{E}_2. \end{cases} \tag{29}$$

Scaling the $\widehat{E}_1^T\Gamma\widehat{E}_1$ and $\widehat{E}_2^T\Gamma\widehat{E}_2$, we obtain the following inequalities:

$$\begin{cases} \widehat{E}_1^T\Gamma\widehat{E}_1 \ge \lambda_{\min}(\Gamma)\sum_{k=1}^{N}\widehat{E}_{1k}{}^2 \ge \lambda_{\min}(\Gamma)\dfrac{1}{\xi_{\max}}\sum_{k=1}^{N}\xi_k\widehat{E}_{1k}{}^2 = \varpi_2\widehat{E}_1^T\Xi\widehat{E}_1, \\ \widehat{E}_2^T\Gamma\widehat{E}_2 \le \lambda_{\max}(\Gamma)\sum_{k=1}^{N}\widehat{E}_{2k}{}^2 \le \lambda_{\max}(\Gamma)\dfrac{1}{\xi_{\min}}\sum_{k=1}^{N}\xi_k\widehat{E}_{2k}{}^2 = \varpi_1\widehat{E}_2^T\Xi\widehat{E}_2. \end{cases} \tag{30}$$

Thus,

$$\dot{V} \le \frac{\dot{\zeta}(t)}{\zeta(t)}\Bigg\{\Bigg[\Bigg(\beta_0-\alpha_1\beta_1+\frac{\beta_0 h+\alpha_1\beta_2}{4\iota_1}\Bigg)\varpi_2 + \beta_1\Bigg(\frac{1}{h}+\alpha_2\Bigg)\frac{1}{4\iota_2}\Bigg]\widehat{E}_1^T\Xi\widehat{E}_1 + \Bigg[\beta_1-\alpha_2\beta_2+\beta_1\Bigg(\frac{1}{h}+\alpha_2\Bigg)\iota_2 + (\beta_0 h+\alpha_1\beta_2)\iota_1\varpi_1\Bigg]\widehat{E}_2^T\Xi\widehat{E}_2\Bigg\}. \tag{31}$$

Furthermore, let $P(t) = \dot{V}(t) + (\eta + \mu(\dot{\zeta}(t)/\zeta(t)))V(t) < 0$. Substituting Equations (26)–(31) into $P(t)$ yields

$$P(t) \le \Bigg(\eta+\mu\frac{\dot{\zeta}(t)}{\zeta(t)}\Bigg)\Big[h\beta_0\widehat{E}_1^T\Gamma\widehat{E}_1 + \beta_2\widehat{E}_2^T\Xi\widehat{E}_2 + \beta_1\widehat{E}_1^T\Xi\widehat{E}_2 + \beta_1\widehat{E}_2^T\Xi\widehat{E}_1\Big] + \frac{\dot{\zeta}(t)}{\zeta(t)}\Bigg\{\Bigg[\Bigg(\beta_0-\alpha_1\beta_1+\frac{\beta_0 h+\alpha_1\beta_2}{4\iota_1}\Bigg)\varpi_2+\beta_1\Bigg(\frac{1}{h}+\alpha_2\Bigg)\frac{1}{4\iota_2}\Bigg]\cdot\widehat{E}_1^T\Xi\widehat{E}_1 + \Bigg[\beta_1-\alpha_2\beta_2+\beta_1\Bigg(\frac{1}{h}+\alpha_2\Bigg)\iota_2+(\beta_0 h+\alpha_1\beta_2)\iota_1\varpi_1\Bigg]\widehat{E}_2^T\Xi\widehat{E}_2\Bigg\}. \tag{32}$$

Scaling $V(t)$, we have

$$V(t) \le \Bigg(h\beta_0+\frac{\beta_1}{2\iota_2}\Bigg)\varpi_1\widehat{E}_1^T\Xi\widehat{E}_1 + (\beta_2+2\beta_1\iota_2)\widehat{E}_2^T\Xi\widehat{E}_2. \tag{33}$$

According to the definitions as Equations (11) and (12), we have $\dot{\zeta}(t)/\zeta(t) \ge h/T$. Substituting it into Equation (33), we have

$$P(t) \le \Bigg\{\frac{h}{T}\Bigg[\Bigg(\beta_0-\alpha_1\beta_1+\frac{\beta_0 h+\alpha_1\beta_2}{4\iota_1}\Bigg)\varpi_2+\beta_1\Bigg(\frac{1}{h}+\alpha_2\Bigg)\cdot\frac{1}{4\iota_2}+\mu\Bigg(h\beta_0+\frac{\beta_1}{2\iota_2}\Bigg)\varpi_1\Bigg]+\eta\Bigg(h\beta_0+\frac{\beta_1}{2\iota_2}\Bigg)\varpi_1\Bigg\}\widehat{E}_1^T\Xi\widehat{E}_1 + \Bigg\{\eta(\beta_2+2\beta_1\iota_2)+\frac{h}{T}\Bigg[\beta_1-\alpha_2\beta_2+\beta_1\Bigg(\frac{1}{h}+\alpha_2\Bigg)\iota_2 + (\beta_0 h+\alpha_1\beta_2)\iota_1\varpi_1+\mu(\beta_2+2\beta_1\iota_2)\Bigg]\Bigg\}\widehat{E}_2^T\Xi\widehat{E}_2. \tag{34}$$

Due to $\eta \ge 0$ and $\mu > 0$, when $2/h \le \mu < -(T/h)(\eta +$

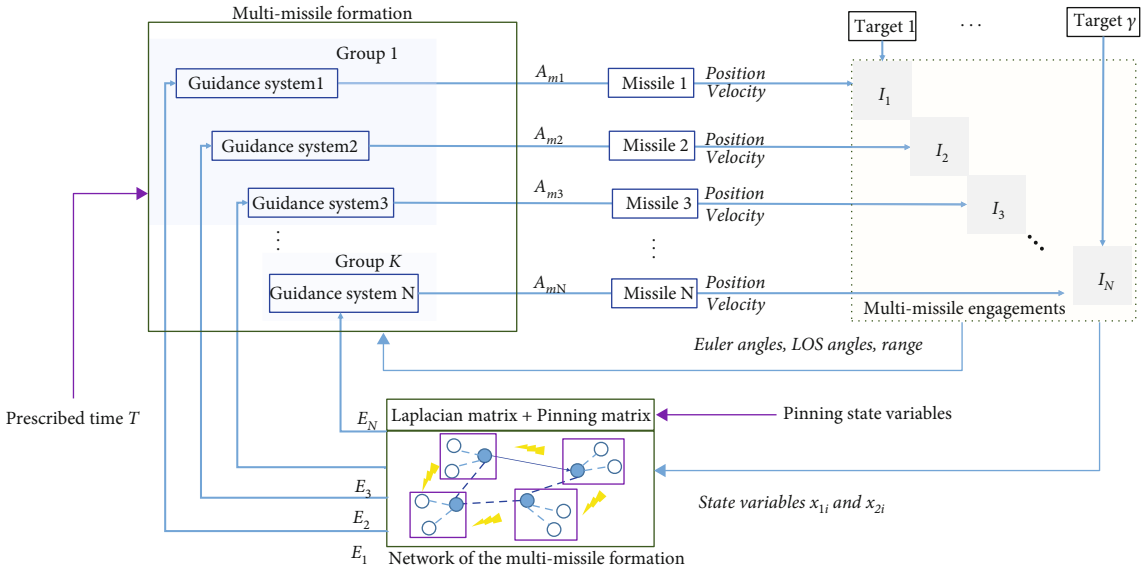

Figure 2: Schematic diagram of prescribed-time cooperative guidance scheme in the first phase.

Input: state variables of the i-th missile and its neighbours, convergence time t_0 and T, group topology $\mathscr{L}$ and pinning scheme D
Output: normal accelerations of the i-th missile in yaw and pitch directions
1. Initialize with initial state of the i-th missile and user prescribed state
2. **When** $t \in [t_0, t_0 + T)$, utilize first-stage cooperative guidance law
3. **If** $|E_1| \le \rho_1, |E_2| \le \rho_2$, switch to the second stage in Step 7.
4. **Else**
5. Gather information of the i-th missile and its neighbours through network
6. Generate the guidance law in Equation (19) with designed gains α_1, α_2, h and ensure the existence of the other virtual parameters.
7. **When** $t \in [t_0 + T, \infty)$, utilize second-stage individual PPN guidance law in Equation (3) with navigation gain K
8. **End**

Algorithm 1: Design steps of local guidance law.

$\max(\Omega_1/\Omega_2, \Omega_3/\Omega_4))$, the parameters satisfy

$$\begin{cases} \dfrac{h}{T}\left[\left(\beta_0 - \alpha_1\beta_1 + \dfrac{\beta_0 h + \alpha_1\beta_2}{4\iota_1}\right)\varpi_2 + \beta_1\left(\dfrac{1}{h} + \alpha_2\right)\dfrac{1}{4\iota_2} + \mu\left(h\beta_0 + \dfrac{\beta_1}{2\iota_2}\right)\varpi_1\right] \\ +\eta\left(h\beta_0 + \dfrac{\beta_1}{2\iota_2}\right)\varpi_1 < 0, \\ \dfrac{h}{T}\left(\beta_1 - \alpha_2\beta_2 + \beta_1\left(\dfrac{1}{h} + \alpha_2\right)\iota_2 + (\beta_0 h + \alpha_1\beta_2)\iota_1\varpi_1 + \mu(\beta_2 + 2\beta_1\iota_2)\right) \\ +\eta(\beta_2 + 2\beta_1\iota_2) < 0. \end{cases} \tag{35}$$

Substituting the inequality Equations (32) and (35) into (34), we have $P(t) < 0$; that is, $\dot{V}(t) \le -(\eta + \mu(\dot{\zeta}(t)/\zeta(t)))V(t)$.

Calculating the inequality $P(t) < 0$, the following inequality holds:

$$V(t) \le \zeta^{-\mu} e^{-\eta(t-t_0)} V(t_0). \tag{36}$$

Moreover, $\dot{\zeta}(t_0)/\zeta(t_0) = h/T$, and letting $\chi = \max(h/T, 1)$, the following inequality can be deduced that

$$\begin{aligned} \widehat{E}_1(t)^2 + \widehat{E}_2(t)^2 &\le \frac{\lambda_{\max}(\Psi)}{\lambda_{\min}(\Psi)}\zeta^{-\mu}\exp^{-\eta(t-t_0)}\left(\widehat{E}_1(t_0)^2 + \widehat{E}_2(t_0)^2\right) \\ &\le \chi^2\frac{\lambda_{\max}(\Psi)}{\lambda_{\min}(\Psi)}\zeta^{-\mu}\exp^{-\eta(t-t_0)}\left(E_1(t_0)^2 + E_2(t_0)^2\right). \end{aligned} \tag{37}$$

Similarly, we have

$$\widehat{E}_1^{\,2} + \widehat{E}_2^{\,2} = \left(\frac{\dot{\zeta}(t)}{\zeta(t)}\right)^2 E_1^{\,2} + E_2^{\,2} \ge \frac{h^2}{T}E_1^{\,2} + E_2^{\,2}. \tag{38}$$

Based on Lemma 5, combining $\widehat{E}_1^{\,2} + \widehat{E}_2^{\,2} \ge 2\widehat{E}_1\widehat{E}_2$ with Equations (37) and (38) obtains

$$\left[\frac{h}{T}E_1(t) + E_2(t)\right]^2 \le 2\chi^2\frac{\lambda_{\max}(\Omega)}{\lambda_{\min}(\Omega)}\zeta^{-\mu}\exp^{-\eta(t-t_0)}[E_1(t_0) + E_2(t_0)]^2. \tag{39}$$

Table 1: Initial conditions of simulation.

Group	No.	(X_I, Y_I, Z_I) (km)	(θ_m, ψ_m) (°)	Group	No.	(X_I, Y_I, Z_I) (km)	(θ_m, ψ_m) (°)
A	1	(-15, 7.5, 2.5)	(10, 4)	C	6	(-15.5, -3.9, 2.5)	(10, -4)
	2	(-13.6, 8.8, 2.8)	(5, 2)		7	(-14.5, -4,3)	(5, -2)
	3	(-11.5, 12, 2.4)	(6 ,3)		8	(-14.5, 2.4, 3)	(4, -3)
B	4	(-15, -4.5, 2.4)	(6, -5)	D	9	(-15, -6.1, 4)	(6, -5)
	5	(-12.5, -21.5, 2.5)	(8, -6)		10	(-14, -16.5, 4)	(8, -6)

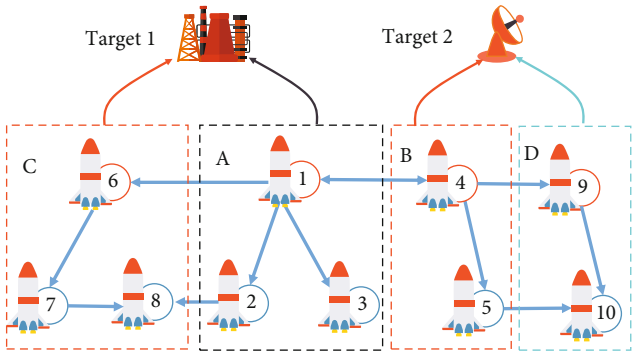

Figure 3: Pinning group network of the 10 missiles with 4 subgroups.

Table 2: Parameters of simultaneous attack.

Setting	Case 1.0	Case 1.1	Case 1.2	Case 1.3	Case 1.4
(α_1, α_2, h)	(1.2, 3, 4)	(2, 4, 4)	(1, 2, 3, 6)	(1.2, 3, 4)	(1.2, 3, 4)
Pinning	1, 4, 6, 9	1, 4, 6, 9	1, 4, 6, 9	1	1, 4, 6, 9
Topology	Figure 3	Figure 3	Figure 3	Figure 3	Figure 9

Therefore, when $t \longrightarrow (t_0 + T)^-$,we have $\zeta^{-\mu} \longrightarrow 0$, so

$$\|E_1(t)\| \longrightarrow 0, \|E_2(t)\| \longrightarrow 0, t \longrightarrow (t_0 + T)^-, \quad (40)$$

that is, $x_{1i} \longrightarrow x_{1,g_i}, x_{2i} \longrightarrow x_{2,g_i}$, which means the pinning group consensus is achieved within the assigned finite time T.

(ii) Keeping pinning group consensus over $[t_0 + T,\infty)$

When $t \in [t_0 + T,\infty), \dot{\zeta}(t)/\zeta(t) = 0$, then

$$\dot{V}(t) \le -\eta V(t) \le 0. \quad (41)$$

Let $t = t_0 + T$; according to Equation (40), it satisfies

$$V(t_0 + T) = \lim_{t \longrightarrow (t_0+T)^-} V(t) = 0. \quad (42)$$

It is obvious that $V(t)$ is continuous at $t = t_0 + T$. Thus,

$$0 \le V(t) \le V(t_0 + T) = 0, \quad \forall t \in [t_0,\infty). \quad (43)$$

That is, $V(t) \equiv 0$ and $E = 0_{2N}$ at any $t \in [t_0 + T,\infty)$. According to the definition of U as Equation (22), we deduce that control input $U \equiv 0_{2N}$ over $[t_0 + T,\infty)$. Hence, the consensus is kept, and the input remains zero over $[t_0 + T,\infty)$ with the guidance law as Equation (19).

(iii) Control input U is bounded and C^0 is smooth over the whole time interval $[t_0, \infty)$

Note that $L_\infty := \{x(t)|x : R_+ \longrightarrow R, \sup_{t \in R_+} |x(t)| < \infty\}$. According to conditions in Theorem 11, $0 < \zeta^{-(1/2)\mu+1/h} \le 1$, $0 < e^{-(1/2)\eta(t-t_0)} \le 1$ hold. Substituting Equation (39) into Equation (22) yields

$$\begin{aligned} \|U\| &= -\alpha_2 \frac{\dot{\zeta}(t)}{\zeta(t)} \widehat{E}_2 - \alpha_1 \left(\frac{\dot{\zeta}(t)}{\zeta(t)}\right)(L + D)\widehat{E}_1 \\ &\le \frac{\dot{\zeta}(t)}{\zeta(t)} \left(\alpha_2 \widehat{E}_2 + \alpha_1 \|L + D\| \widehat{E}_1\right) \le \frac{\dot{\zeta}(t)}{\zeta(t)} \max\left(\alpha_2, \alpha_1 \|L + D\|\right) \\ &\cdot \left(\widehat{E}_2 + \widehat{E}_1\right) \le \sqrt{2}\chi \frac{h}{T} \sqrt{\frac{\lambda_{\max}(\Omega)}{\lambda_{\min}(\Omega)}} \max\left(\alpha_2, \alpha_1 \|L + D\|\right) \\ &\cdot \zeta^{-(1/2)\mu+1/h} \exp^{-(1/2)\eta(t-t_0)} [E_1(t_0) + E_2(t_0)]. \end{aligned} \quad (44)$$

According to the proof, in Equations (41) and (46), the input is C^0 smooth over the whole time interval. Besides, the control input remains zero over $[t_0 + T,\infty)$ and is bounded over $[t_0, t_0 + T)$. So it is obvious that U is bounded over $[t_0, \infty)$.

According to the three parts, the multimissiles can realize consensus at the prescribed time with the pinning group guidance law. Therefore, the group prescribed-time cooperative guidance law Equation (19) can ensure that the multimissile system Equation (14) will achieve the group prescribed-time cooperative attack. This completes the proof. □

Remark 12. Different from most of existing results of finite-time or fixed-time cooperative guidance law by estimating the upper bound of settling time, the settling time of the proposed cooperative guidance law (19) can be assigned off-line according to interception mission requirements without estimation. Besides, compared with existing conservative group consensus, the pinning scheme helps to transform the special communication conditions into general coupling topology considering the interaction between groups.

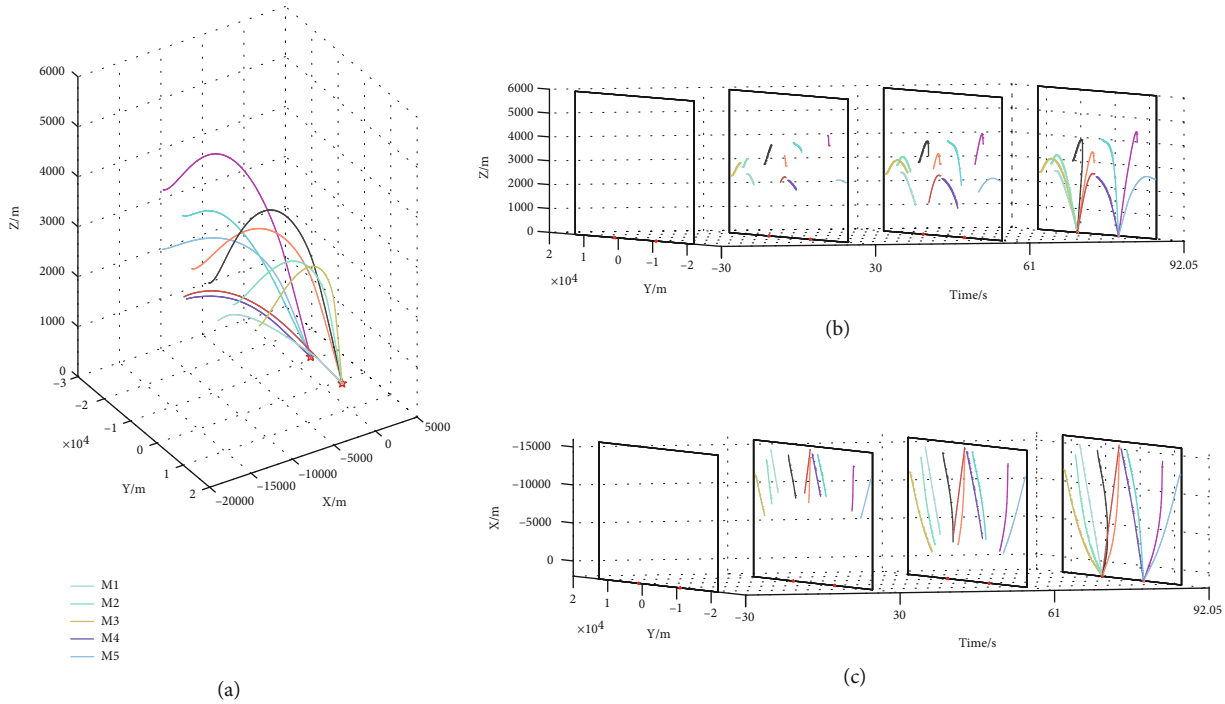

Figure 4: Trajectory of Case 1.0: (a) 3-D trajectory; (b) trajectory on Y-Z plane; (c) trajectory on X-Y plane.

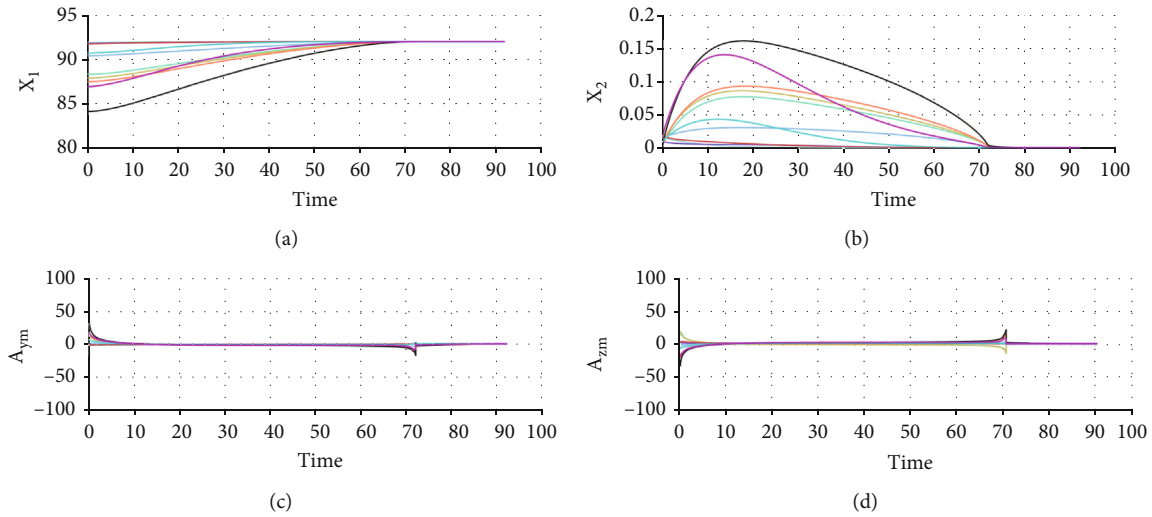

Figure 5: Variables of Case 1.0: (a) state variable x_1; (b) state variable x_2; (c) normal command A_{ym}; (d) lateral Command A_{zm}.

Remark 13. Parameters or matrices in Theorem 11 can be divided into four types for designing easily as follows: (i) system matrices $\mathscr{L}$ and D. $\mathscr{L}$ and D represent the topology of multimissiles, which are decided by structure of communication network and missile's task orientation. Generally, $\mathscr{L}+D$ must be a M-matrix. (ii) Convergence parameters T and h. T is prescribed as the convergence time based on the requirements of the mission or users, and h strongly affects the convergence rate by adjusting the gain variation. (iii) Guidance gains α_1 and α_2 need to be designed, which are strongly associated with the stability of the system. (iv) The others are process parameters and matrices. Matrices Ξ and Γ related to the network must to satisfy the properties of the M-matrix. Lyapunov parameters β_0, β_1, and β_2 are given to guarantee the $\Psi > 0$. Prescribed-time convergence parameters are η and μ. Scaling parameters are ι_1 and ι_2.

According to the structure of the system and user's requirements, the first three types of parameters need to be designed or assigned. The other parameters and matrices are process parameters which only need to exist.

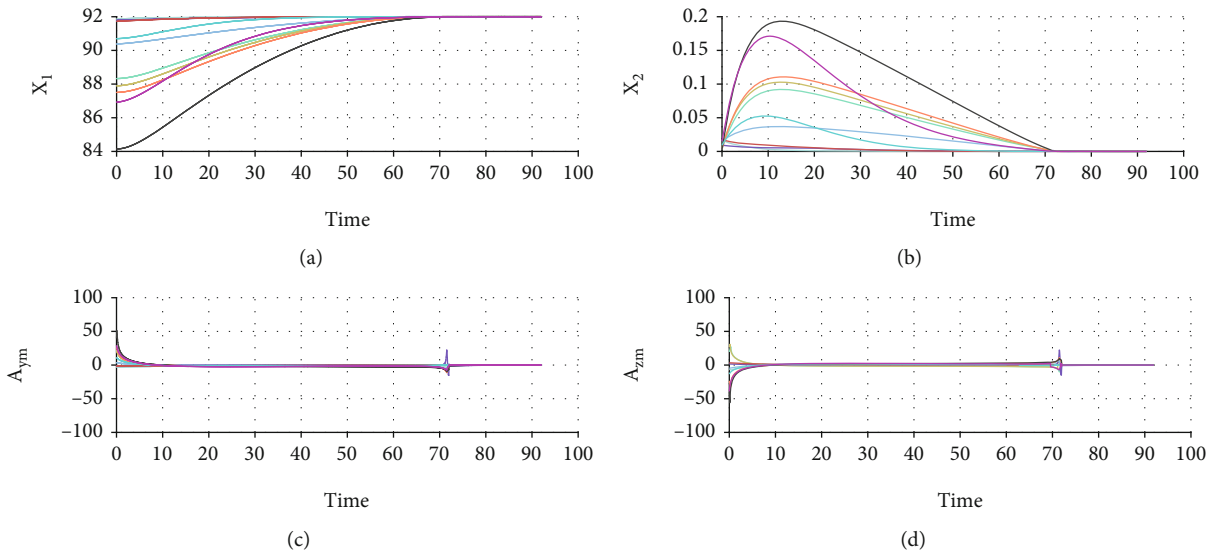

Figure 6: Variables of Case 1.1: (a) state variable x_1; (b) state variable x_2; (c) normal command A_{ym}; (d) lateral command A_{zm}.

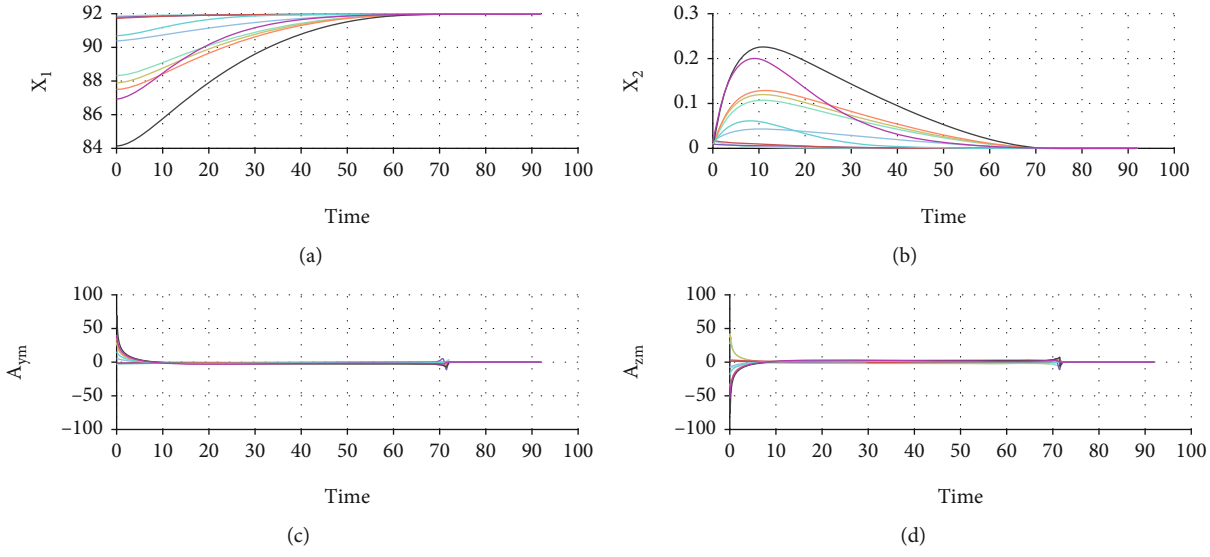

Figure 7: Variables of Case 1.2: (a) state variable x_1; (b) state variable x_2; (c) normal command A_{ym}; (d) lateral command A_{zm}.

Remark 14. The group's impact time t_{f,g_i} need to satisfy

$$t_{f,g_i} \geq \max\left(t_{f,i}\right), \quad i \in \boldsymbol{g}_{g_i}. \tag{45}$$

When the missile flies to the target with $\sigma_i = 0$, its arrival time is the shortest. If the t_{f,g_i} is shorter than its estimation, it is impossible for the i-th missile to cooperate with others. Hence, the latest missile in subgroup should be pinned first.

3.2. Practical Implementation. Compared with the existing researches, the proposed prescribed-time pinning group consensus-based cooperative guidance law has two advantages: faster convergence speed and fewer restrictions. Firstly, the convergence time can be arbitrarily specified, instead of retuning parameters to obtain an upper boundary. Secondly, the proposed cooperative guidance law is not only independent of initial conditions but also relaxing the convergence condition by the pinning group network. For targets protected by strong defensive interference, the relaxed restrictions and earlier convergence are beneficial for intercepting. The diagram of the proposed prescribed-time cooperative guidance scheme is given in Figure 2.

However, the application of proposed guidance law faces a common problem; that is, it cannot satisfy the precise consensus convergence property but the bounded error consensus. Though the virtual constructed state variables are selected as information transmitted by physical network communication, they are strongly connected with actual physical state of missile and influence the guidance precision. Actually, in many practical interception missions, the bounded error consensus convergence is common. Hence, the objective of prescribed-time cooperative guidance law is to reduce the group

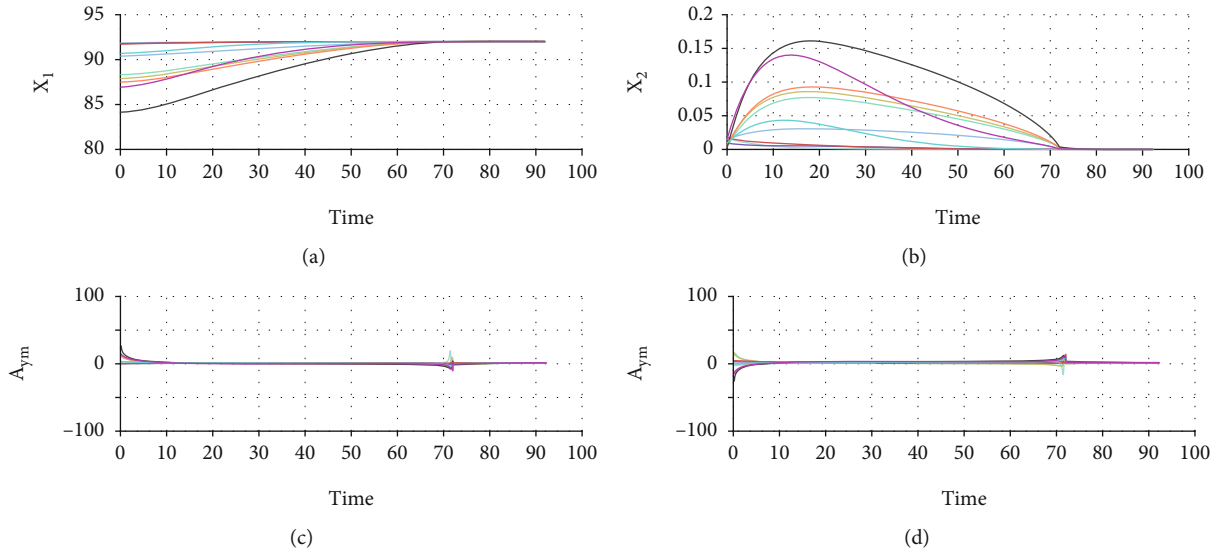

Figure 8: Variables of Case 1.3: (a) state variable x_1; (b) state variable x_2; (c) normal Command A_{ym}; (d) lateral command A_{zm}.

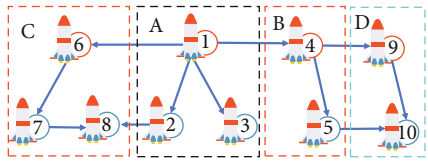

Figure 9: Topology of Case 1.4.

consensus error less than the given boundaries ρ_1 and ρ_2, which represent the lower limits of allowable errors for multi-missiles achieving cooperation tasks.

In order to make full use of the superiority of the proposed cooperative guidance law, the two-stage cooperative guidance scheme can be given for simultaneous interception. Decided by the mission, the prescribed convergence time provides a clear switching point. Meanwhile, combining with the analysis of Equations (5)–(7), individual PPN can achieve the cooperative interception with convergent cooperative state variables, which helps to avoid communication problems in hostile areas. Besides, taking the prescribed convergence instant as the switching point, the PPN in the second stage can significantly reduce the cost and interference in network communication.

On this basis, the implementable version of the practical two-stage cooperative guidance scheme is summarized and the design steps are given as follows.

In the following, we give an explanation about the design steps.

Firstly, a prescribed-time cooperative guidance law in Equation (19) is utilized to achieve agreement of the range-to-go and heading angle through the constructed state variables.

Secondly, when the errors of state variables satisfy the conditions $|E_1| \le \rho_1$ and $|E_2| \le \rho_2$,if $t \in [t_0, t_0 + T)$, then the cooperative guidance commands are switched into individual PPN guidance law outlined in Equation (3). Otherwise, the switching will be executed when time comes to the prescribed convergence instant $t_0 + T$.

Remark 15. Note that unsuitable small values of boundaries are not conducive to the switching between the two stages, even leading to failure of mission.

Remark 16. To overcome the inherent singularity problem, a small boundary layer is given for Equation (19). Suppose that there exist small constants r_{lower}, d_1, and d_2, then the prescribed-time cooperative guidance law can be rewritten as

$$\begin{cases} A_{ymi\_co} = -\dfrac{V_M^2}{r_{i\_\lim}} \sin \psi_{mi} + \dfrac{U_i V_M}{Q_1}, \\ A_{zmi\_co} = -\dfrac{V_M^2}{r_{i\_\lim}} \sin \theta_{mi} \cos \psi_{mi} + \dfrac{U_i V_M}{Q_2}, \end{cases} \tag{46}$$

where $r_{i\_\lim} = \max(r_i, r_{lower})$ and r_{lower} is the selected near miss-distance; $Q_1 = \max(2 \sin \psi_{\mathrm{Mi}}, d_1 \operatorname{sgn}(\sin \psi_{Mi}))$ and $Q_2 = \max(2 \sin \theta_{\mathrm{Mi}} \cos \psi_{Mi}, d_2 \operatorname{sgn}(\sin \theta_{Mi} \cos \psi_{Mi}))$, in which d_1 and d_2 are strongly related to limitations of heading error. Though the influence of modification is passive for the prescribed-time convergence, it will only work when time is very close to the specified time $t_0 + \mathrm{T}$. Besides, if d_1 and d_2 are small enough, the influence can be ignored.

Remark 17. With the prescribed-time scaling function, the proposed prescribed-time cooperative guidance can achieve convergence at a specified time. However, for its continuously growing gains, if the convergence errors are not small enough, rapidly increasing commands at the end of terminal guidance are not beneficial for the actuator working with maximum overload. In theory, the prescribed-time consensus can be ensured. Nevertheless, considering the complex environment and performance in practice, smaller and smoother overloads are beneficial. In order to improve the practicability of the proposed cooperative guidance law, the two-stage cooperative guidance law is given to avoid the

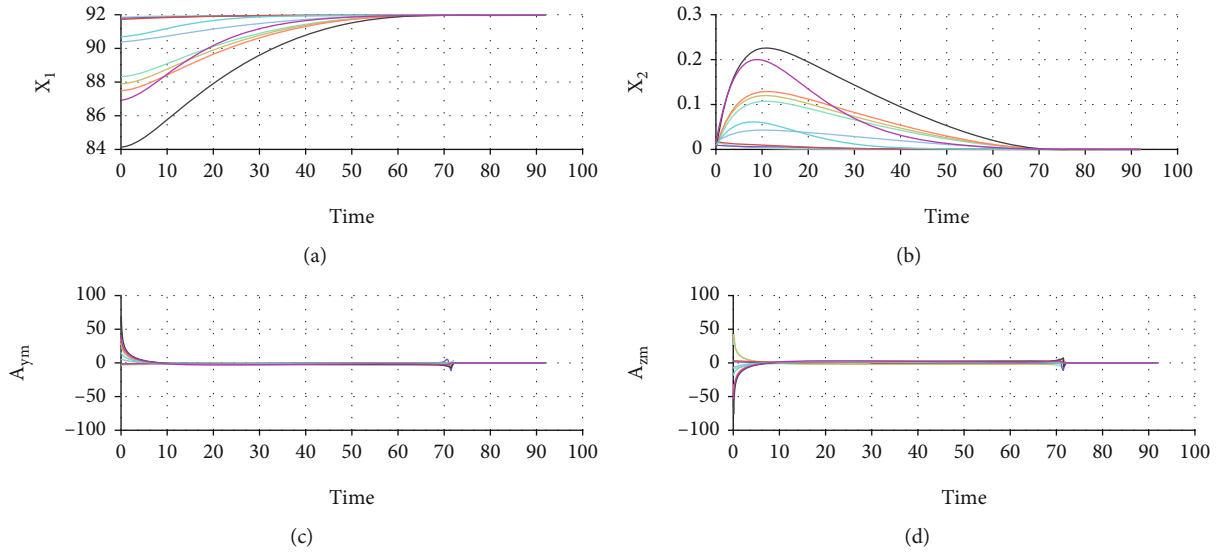

Figure 10: Variables of Case 1.4 with one directed spanning tree: (a) state variable x_1; (b) state variable x_2; (c) normal command A_{ym}; (d) lateral command A_{zm}.

greatly increasing command as the prescribed-time approaches. On the first stage, the prescribed-time cooperative guidance law is used for group convergence of state variables and the PPN takes over in the second stage. However, the hard switching scheme at specified time T may cause sudden changes for guidance command, which leads to difficulties for implementation of actuators. Hence, the soft switching scheme with the weight function is given as follows:

$$w = \left(\frac{T + t_0 - t}{T + t_0 - t_d}\right)^l, \tag{47}$$

where t_d is a small transition time for switching which satisfies $t_0 \le t_d \le t_0 + T$ and $l \ge 1$.

According to the Equations (3), (19), (46), and (47), the switching guidance law is given as

$$A_{ymi} = \begin{cases} A_{ymi\_co}, t \in [t_0, T + t_0 - t_d), \\ wA_{ymi\_co} + (1 - w)A_{ymi\_PPN}, t \in [T + t_0 - t_d, T + t_0), \\ A_{ymi\_PPN}, t \in [T + t_0, \infty), \end{cases}$$
$$A_{zmi} = \begin{cases} A_{zmi\_co}, t \in [t_0, T + t_0 - t_d), \\ wA_{zmi\_co} + (1 - w)A_{zmi\_PPN}, t \in [T + t_0 - t_d, T + t_0), \\ A_{zmi\_PPN}, t \in [T + t_0, \infty). \end{cases} \tag{48}$$

Remark 18. At the second stage of terminal guidance, losing the target will cause the failure of task. Thus, cooperation with better view field can provide more schemes. When $t \longrightarrow (t_0 + T)^-$, then $\zeta(t) \longrightarrow \infty$, considering the little state errors; though the adaption time-varying gain helps to achieve convergence, it may also lead to too much overload for the prescribed-time convergence. Selecting a short time period for soft switching can ensure the smooth handoff without affecting cooperative guidance

Table 3: Consumption evaluation indicators of Case 1.

J	Case 1.0	Case 1.1	Case 1.2	Case 1.3	Case 1.4
J_y	1108	1207	1264	1133	1109
J_z	1154	1209	1250	1189	1165

4. Simulation and Analysis

In this section, the simulations were carried out to demonstrate the performance of the proposed 3-D two-stage prescribed-time cooperative guidance law for different scenarios. Three scenarios for describing multiple missiles against multiple stationary targets are given.

For verification, the initial conditions of a missile group including 10 missiles with 4 subgroups attack two stationary targets are given in Table 1, where four subgroups are denoted as A to D for convenient expression. The target of group A and C is located at $(2\,\text{km}, 1\,\text{km}, 0\,\text{km})$ and the target of group B and D is located in $(2\,\text{km}, -11\,\text{km}, 0\,\text{km})$. The constant speed of the missile is 200 m/s. The navigation gain of PPN is set as $K = 4$. Besides, for the proposed cooperative guidance law the time interval t_d is given as 0.5 s, l is 2, d_1 and d_2 are both 0.01, ρ_1 and ρ_2 are 0.1 and 0.01, respectively. The limitation manoeuvring overload of actuators is ±10 g.

On this basis, the network of the 10-missile group is shown in Figure 3.

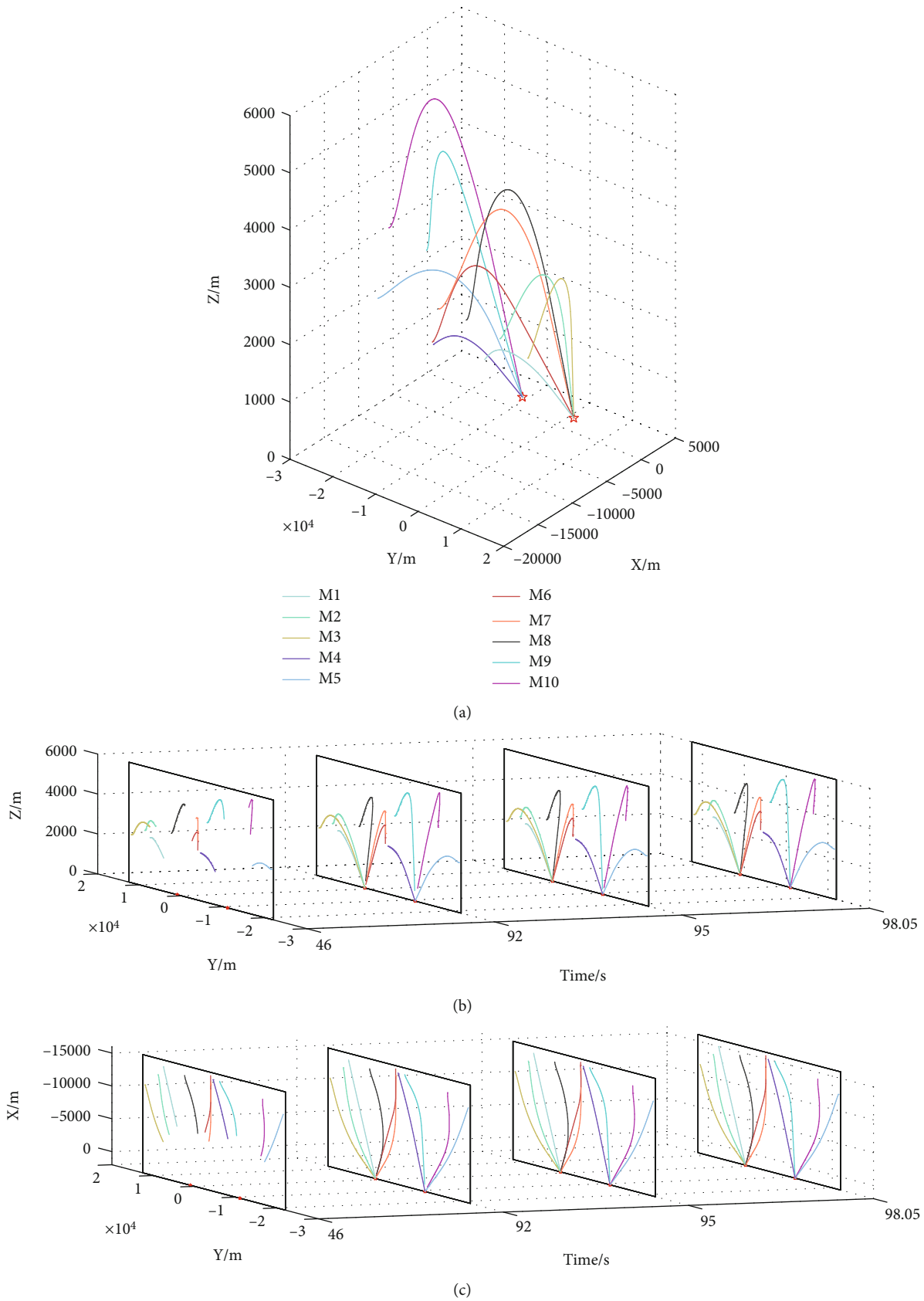

Figure 11: Trajectory of Case 2: (a) 3-D trajectory; (b) trajectory on Y-Z plane; (c) trajectory on X-Y plane.

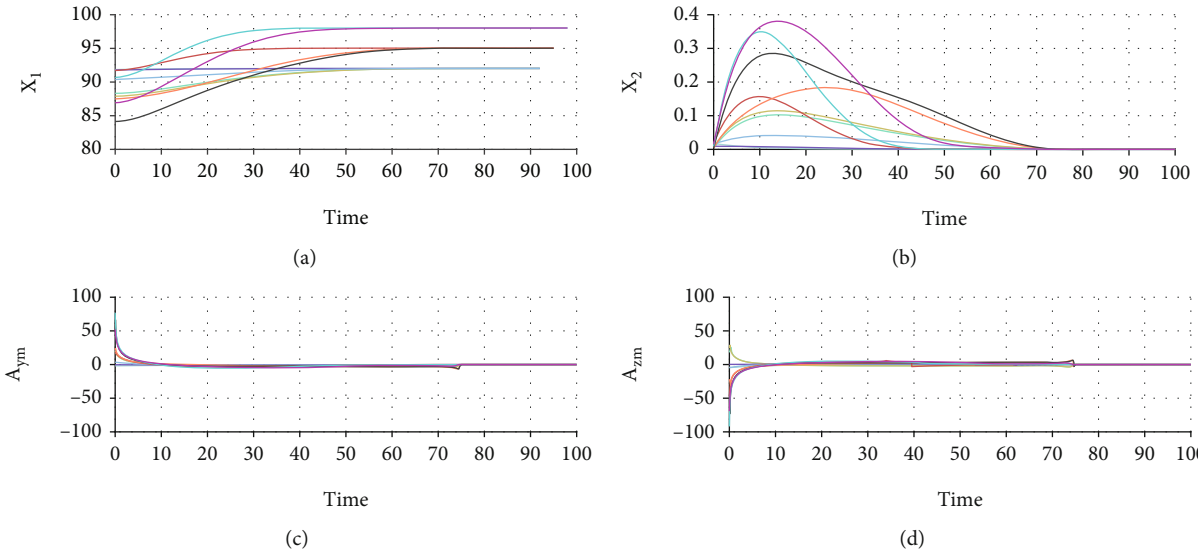

FIGURE 12: Variables of Case 2 with one directed spanning tree: (a) state variable x_1; (b) state variable x_2; (c) normal command A_{ym}; (d) lateral command A_{zm}.

Hence, the Laplacian matrix can be written as

$$L = \begin{bmatrix} 1 & 0 & 0 & -1 & 0 & 0 & 0 & 0 & 0 & 0 \\ -1 & 1 & 0 & 0 & 0 & 0 & 0 & 0 & 0 & 0 \\ -1 & 0 & 1 & 0 & 0 & 0 & 0 & 0 & 0 & 0 \\ -1 & 0 & 0 & 1 & 0 & 0 & 0 & 0 & 0 & 0 \\ 0 & 0 & 0 & -1 & 1 & 0 & 0 & 0 & 0 & 0 \\ -1 & 0 & 0 & 0 & 0 & 1 & 0 & 0 & 0 & 0 \\ 0 & 0 & 0 & 0 & 0 & -1 & 1 & 0 & 0 & 0 \\ 0 & -1 & 0 & 0 & 0 & 0 & -1 & 2 & 0 & 0 \\ 0 & 0 & 0 & -1 & 0 & 0 & 0 & 0 & 1 & 0 \\ 0 & 0 & 0 & 0 & -1 & 0 & 0 & 0 & -1 & 2 \end{bmatrix}, \tag{49}$$

and the pinning matrix is written as $D = \text{diag}([1\,0\,0\,1\,0\,1\,0\,0\,1\,0])$,where missiles 1, 4, 6, and 9 are pinned, which means at least one node in each group is pinned while inter-subgroup communication is kept in all cases. The Laplacian matrix shows that the topology in Figure 3 contains two directed spanning trees with nodes 1 and 4 as root.

The control variables represent the energy consumption. For actuators' limitation, smaller control variables are favourable for application. Consumption evaluation indicators are defined as follows.

$$J_i = \int_0^t |u_i(t)|dt, J = \sum_{i=1}^{N} J_i. \tag{50}$$

4.1. Case 1: Simultaneous Attack. Considering a simultaneously engagement scenario, the prescribed convergence time is set as 72 s and all the subgroups' pinned state variables are expected as 92 and 0. To analyze the influence of guidance gains, verifications were conducted on the 5 cases shown in Table 2.

4.1.1. Case 1.0. The simulation results of Case 1.0, including trajectory, state variables, and acceleration commands, are presented in Figures 4 and 5. With demonstration of Case 1, the simultaneously attack for different targets is achieved with arrival time error within 0.01 s. Figure 5 shows that the convergence is achieved at the prescribed time with two-stage switching permissible error and the control commands are less than 40 m/s^2, which keeps within bounds of the actuators. Pinning state variable $x_{2,g_i} = 0$ means that the velocity coincides with the line-of-sight; x_1 represents the arrival time after the prescribed time. Since the convergences of state variables are interactional, the errors of x_2 lead to the error of actual arrival time. Besides, the transient switching process balancing the excessive control command also has a certain impact on it. Furthermore, taking the relationship between virtual state variables and actual arrival time into consideration, it is reasonable to scatter the arrival time between 92.01 s and 92.02 s.

4.1.2. Cases 1.1–1.4. The simulation results of Cases 1.1–1.3 are shown in Figures 6–8. We choose one of the spanning directed trees with zero-in-degree node 1 in Figure 9 and keep the pinning scheme for Case 1.4; the variables are shown in Figure 10.

4.1.3. Simulation Analysis of Case 1. The consumption evaluation indicators are shown in Table 3. Taking Case 1.0 as a reference, further analysis is given as follows.

The first three cases have shown the influence of control command. Compared with Case 1.1, though the larger control commands increase the convergence rate and reduce the error of state variables, larger overshoots which may cause the heading angles likely exceed the physical limitations of

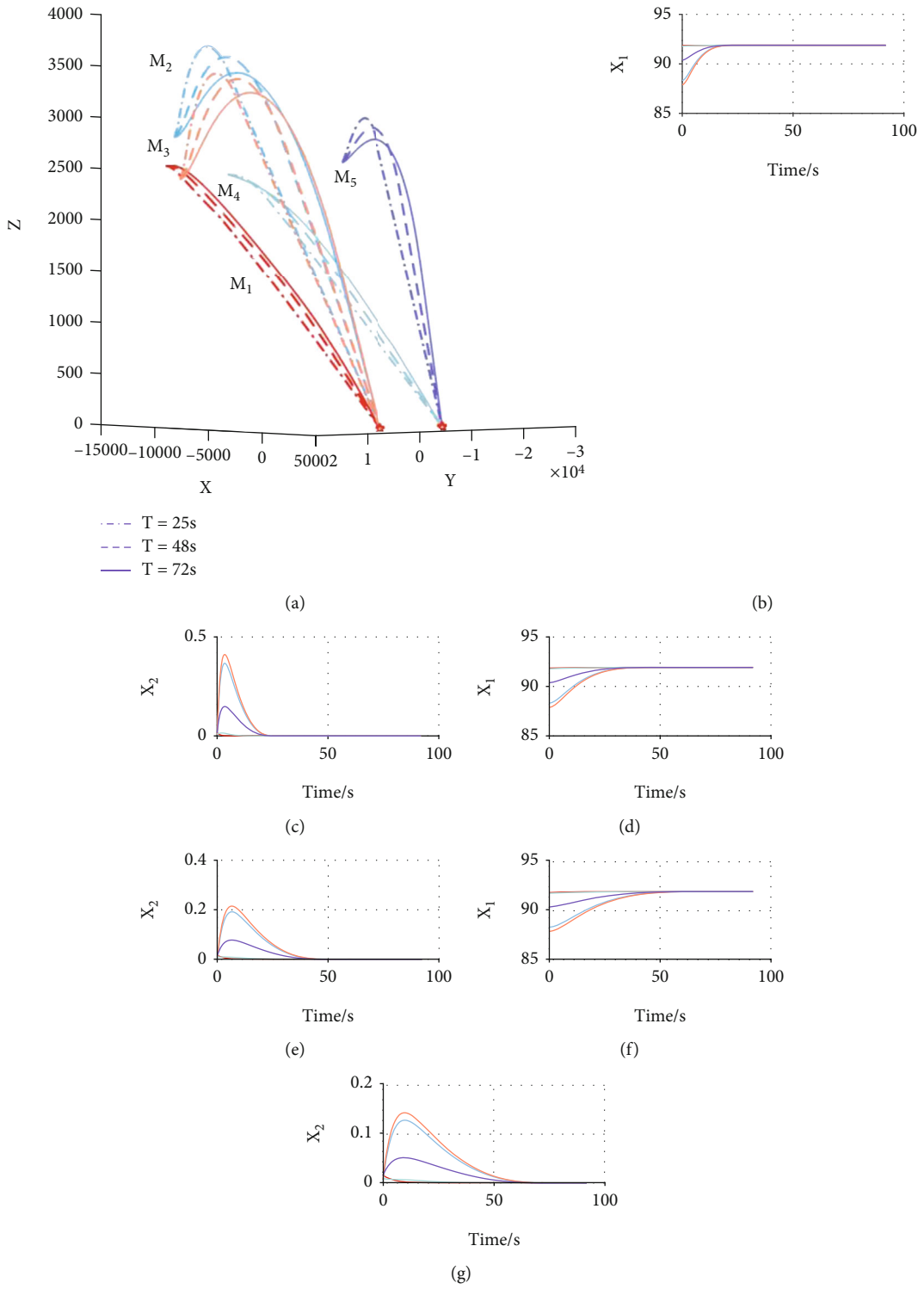

FIGURE 13: Comparison of prescribed convergence time: (a) 3-D trajectory; (b) $T = 25$ s,state variable x_1; (c) $T = 25$ s, state variable x_2; (d) $T = 48$ s, state variable x_1; (e) $T = 48$ s, state variable x_2; (f) $T = 72$ s, state variable x_1; (g) $T = 72$ s, state variable x_2.

seekers. In Case 1.2, h is the pow parameter of the prescribed-time function; its increase greatly affects the control commands. Compared with the increase of gains, the increase of the pow is advantageous to decrease the control commands before the two-stage switching. However, the larger the pow is, the larger initial control commands are needed for prescribed-time convergence.

With the same control gains, the influence of pinning group topology is analyzed. In Case 1.3, node 1 is only the pinned node; the control commands have a chattering

property which has adverse effect on stability. As for Case 1.4, one directed spanning tree causes more consumption.

Although bigger gains or pow is beneficial to increasing the convergence speed, more consumption is needed. Besides, the structure of the communication network is also essential. When the pinning group scheme satisfies the M -matrix, the simpler the network connected, the more energy consumption of control is needed for the more incomplete information. Accordingly, striking a balance between the network communication complexity and available cooperative guidance command is required under different circumstances when selecting the control parameters and pinning group scheme.

4.2. Case 2: Time-Difference Attack on the Same Target with Different Intervals. This case is given for possible scenarios of round attack. Viewing each subgroup as a round unit, the round attack can be achieved by the proposed pinning group cooperative guidance law with different time intervals. The prescribed convergence time is set at 75 s, and all the pinned virtual state variables $x_{2,g_i} = 0$. For the round attack on the first target, pinned state variables of subgroups A and C are 92 s and 98 s, respectively. As to the round attack on the second target, pinned state variables of subgroups B and D are 92 s and 98 s, respectively. To achieve the simultaneous attack, the parameters are given as follows: $\alpha_1 = 2$, $\alpha_2 = 3.3$, and $h = 4$. The simulation results of are presented in Figures 11 and 12.

The simulation results show that when subgroups A and B reach their respective targets at the same time, subgroups A and C achieve round attack with a time difference of 3 s. Similarly, the time difference between subgroups B and D attacking the second target is 5 s. With intrasubgroup arrival time error less than 0.01 s, the subgroup D arrives at 98.027 s, subgroup C arrives at 95.03 s, and subgroups A and C arrive at 92.02 s. For the mission of round attack, the absolute values of initial control commands are less than $\pm 10g$ which are caused by initial errors of state variables and control gains. However, the commands are acceptable for the actuators. Considering good extensibility of the proposed pinning group scheme, it benefits to realize large scale multimissiles' round attack.

4.3. Case 3: Comparison of Prescribed Convergence Time. Case 3 is given for showing the advantages of prescribed-time cooperative guidance law by comparisons. Considering the cooperation between Group A and Group B with different assigned convergence times, the control parameters are set as$\alpha_1 = 1.5$, $\alpha_2 = 3$, and $h = 6$.

To demonstrate the effectiveness of proposed scheme, the prescribed times for the switching stage are appointed as 25 s, 48 s, and 72 s.

According to the simulation results in Figure 13, the switching time can be arbitrarily assigned with proper control parameters, and the cooperation can be achieved regardless of the specified time. Specified time consensus achieved at the prescribed time in the first stage for providing ideal conditions for the second stage.

5. Conclusions

This paper has proposed a 3-D two-stage prescribed-time pinning group cooperative guidance law for supporting different attacking scenarios of multimissiles. In the first stage, the prescribed-time convergence of the proposed pinning group consensus-based cooperative guidance law has been proven. With the proposed cooperative guidance law, each missile will lock on its subgroups' target with expected cooperative range-to-go at the specified convergence time. Cooperating with the expected subgroups' heading error and range-to-go, the cooperative guidance law switches to the second stage. In the second stage, the PPN has been employed to lead the cooperating missiles in the same subgroup to impact on the target. Based on the synergy of the pinning group prescribed-time two-stage cooperative guidance law, one subgroup can reach any specified target with reasonable engagement, and its convergence time can be assigned, which provides possibilities for the target fire distribution. Simulations have validated the effectiveness of the proposed cooperative guidance law. On this basis, this work presented in this paper can be further extended in the case of manoeuvring target interception.

Data Availability

The data used to support the findings of this study are included within the article.

Conflicts of Interest

The authors declared that they have no conflicts of interest in this work.

Acknowledgments

The authors are grateful for the support provided by the National Natural Science Foundation of China (Grant Nos. 61973253, 62006192, and 62176214).

References

[1] S. He and D. Lin, "Three-dimensional optimal impact time guidance for antiship missiles," *Journal of Guidance, Control, and Dynamics*, vol. 42, no. 4, pp. 941–948, 2019.

[2] X. Chen and J. Wang, "Nonsingular sliding-mode control for field-of-view constrained impact time guidance," *Journal of Guidance, Control, and Dynamics*, vol. 41, no. 5, pp. 1214–1222, 2018.

[3] S. Liu, B. Yan, T. Zhang, P. Dai, and J. Yan, "Guidance law with desired impact time and FOV constrained for antiship missiles based on equivalent sliding mode control," *International Journal of Aerospace Engineering*, vol. 2021, Article ID 9923332, 15 pages, 2021.

[4] in-Soo Jeon, Jin-Ik Lee, and Min-Jea Tahk, "Impact-time-control guidance law for anti-ship missiles," *IEEE Transactions on Control Systems Technology*, vol. 14, no. 2, pp. 260–266, 2006.

[5] J. I. Lee, I. S. Jeon, and M. J. Tahk, "Guidance law to control impact time and angle," *IEEE Transactions on Aerospace and Electronic Systems*, vol. 43, no. 1, pp. 301–310, 2007.

[6] I. S. Jeon and J. I. Lee, "Homing guidance law for cooperative attack of multiple missiles," *Journal of Guidance, Control, and Dynamics*, vol. 33, no. 1, pp. 275–280, 2010.

[7] S. Y. Zhao and R. Zhou, "Cooperative guidance for multimissile salvo attack," *Chinese Journal of Aeronautics*, vol. 21, no. 6, pp. 533–539, 2008.

[8] S. Y. Zhao, R. Zhou, and W. Chen, "Design of time-constrained guidance laws via virtual leader approach," *Chinese Journal of Aeronautics*, vol. 23, no. 1, pp. 103–108, 2010.

[9] E. Zhao, S. Wang, T. Chao, and M. Yang, "Multiple missiles cooperative guidance based on leader-follower strategy," in *Proceedings of 2014 IEEE Chinese Guidance, Navigation and Control Conference, 2014; 2014 Aug 8-10*, pp. 1163–1167, Yanta,China, 2014.

[10] A. Sinha and S. R. Kumar, "Supertwisting control-based cooperative salvo guidance using leader–follower approach," *IEEE Transactions on Aerospace and Electronic Systems*, vol. 56, no. 5, pp. 3556–3565, 2020.

[11] Q. Zhao, X. Dong, Z. Liang, C. Bai, J. Chen, and Z. Ren, "Distributed cooperative guidance for multiple missiles with fixed and switching communication topologies," *Chinese Journal of Aeronautics*, vol. 30, no. 4, pp. 1570–1581, 2017.

[12] Y. A. Zhang, X. L. Wang, and H. L. Wu, "A distributed cooperative guidance law for salvo attack of multiple anti-ship missiles," *Chinese Journal of Aeronautics*, vol. 28, no. 5, pp. 1438–1450, 2015.

[13] X. L. Wang, Y. A. Zhang, and H. L. Wu, "Distributed cooperative guidance of multiple anti-ship missiles with arbitrary impact angle constraint," *Aerospace Science and Technology*, vol. 46, pp. 299–311, 2015.

[14] Y. A. Zhang, G. X. Ma, and A. L. Liu, "Guidance law with impact time and impact angle constraints," *Chinese Journal of Aeronautics*, vol. 26, no. 4, pp. 960–966, 2013.

[15] Y. A. Zhang, X. L. Wang, and H. L. Wu, "Impact time control guidance law with field of view constraint," *Aerospace Science and Technology*, vol. 39, pp. 361–369, 2014.

[16] X. F. Wang, Y. W. Zhang, D. Z. Liu, and M. He, "Three-dimensional cooperative guidance and control law for multiple reentry missiles with time-varying velocities," *Aerospace Science and Technology*, vol. 80, pp. 127–143, 2018.

[17] Y. Chen, J. Wang, J. Shan, and M. Xin, "Cooperative guidance for multiple powered missiles with constrained impact and bounded speed," *Journal of Guidance, Control, and Dynamics*, vol. 44, no. 4, pp. 825–841, 2021.

[18] T. Lyu, Y. Guo, C. Li, G. Ma, and H. Zhang, "Multiple missiles cooperative guidance with simultaneous attack requirement under directed topologies," *Aerospace Science and Technology*, vol. 89, no. 6, pp. 100–110, 2019.

[19] Z. Wu, Q. Ren, Z. Luo, Y. Fang, and W. Fu, "Cooperative midcourse guidance law with communication delay," *International Journal of Aerospace Engineering*, vol. 2021, Article ID 3460389, 16 pages, 2021.

[20] S. Zhang, Y. Guo, Z. Liu, S. Wang, and X. Hu, "Finite-time cooperative guidance strategy for impact angle and time control," *IEEE Transactions on Aerospace and Electronic Systems*, vol. 57, no. 2, pp. 806–819, 2021.

[21] J. Zeng, L. Dou, and B. Xin, "A joint mid-course and terminal course cooperative guidance law for multi-missile salvo attack," *Chinese Journal of Aeronautics*, vol. 31, no. 6, pp. 1311–1326, 2018.

[22] S. R. Kumar and D. Mukherjee, "Cooperative salvo guidance using finite-time consensus over directed cycles," *IEEE Transactions on Aerospace and Electronic Systems*, vol. 56, no. 2, pp. 1504–1514, 2020.

[23] S. He, W. Wang, D. Lin, and H. Lei, "Consensus-based two-stage salvo attack guidance," *IEEE Transactions on Aerospace and Electronic Systems*, vol. 54, no. 3, pp. 1555–1566, 2018.

[24] W. DONG, Q. WEN, Q. XIA, and S. YANG, "Multiple-constraint cooperative guidance based on two-stage sequential convex programming," *Chinese Journal of Aeronautics*, vol. 33, no. 1, pp. 296–307, 2020.

[25] Z. Li and Z. Ding, "Robust cooperative guidance law for simultaneous arrival," *IEEE Transactions on Control Systems Technology*, vol. 27, no. 3, pp. 1360–1367, 2019.

[26] S. H. Song and I. J. Ha, "A Lyapunov-like approach to performance analysis of 3-dimensional pure PNG laws," *IEEE Transactions on Aerospace and Electronic Systems*, vol. 30, no. 1, pp. 238–248, 1994.

[27] S. M. He, M. Kim, T. Song, and D. F. Lin, "Three-dimensional salvo attack guidance considering communication delay," *IEEE Transactions on Aerospace and Electronic Systems*, vol. 73, no. 2, pp. 1–9, 2018.

[28] Y. Chen, J. Wang, C. Wang, J. Shan, and M. Xin, "Three-dimensional cooperative homing guidance law with field-of-view constraint," *Journal of Guidance, Control, and Dynamics*, vol. 43, no. 5, pp. 1–9, 2019.

[29] X. H. Wang and C. P. Tan, "3-D impact angle constrained distributed cooperative guidance for maneuvering targets without angular-rate measurements," *Control Engineering Practice*, vol. 78, no. 9, pp. 142–159, 2018.

[30] X. H. Wang and X. Lu, "Three-dimensional impact angle constrained distributed guidance law design for cooperative attacks," *ISA Transactions*, vol. 73, pp. 79–90, 2018.

[31] X. Xu, C. Chen, Z. Ren, and S. Li, "Multiple tactical missiles cooperative attack with formation-containment tracking requirement along the planned trajectory," *IEEE Access*, vol. 8, pp. 87929–87946, 2020.

[32] J. Zhao and S. Yang, "Integrated cooperative guidance framework and cooperative guidance law for multi-missile," *Chinese Journal of Aeronautics*, vol. 31, no. 3, pp. 546–555, 2018.

[33] Q. Zhao, X. Dong, J. Chen, Z. Xiong, Q. Li, and Z. Ren, "Group cooperative guidance for multiple missiles with directed topologies," in *2016 35th Chinese control conference (CCC); 2016 Jul 27-29*, pp. 5699–5704, IEEE, Chengdu, China, 2016.

[34] Q. Zhao, X. Dong, Z. Liang, and Z. Ren, *Distributed group cooperative guidance for multiple missiles with switching directed communication topologies*, 2017 36th Chinese Control Conference (CCC), 2017; 2017 July 26-28, Dalian, China, 2017.

[35] Q. Zhao, X. Dong, Z. Liang, and Z. Ren, "Distributed group cooperative guidance for multiple missiles with fixed and switching directed communication topologies," *Nonlinear Dynamics*, vol. 90, no. 4, pp. 2507–2523, 2017.

[36] J. H. Song, S. M. Song, and S. L. Xu, "Three-dimensional cooperative guidance law for multiple missiles with finite-time convergence," *IEEE Transactions on Aerospace and Electronic Systems*, vol. 67, pp. 193–205, 2017.

[37] G. Li, Y. Wu, and P. Xu, "Adaptive fault-tolerant cooperative guidance law for simultaneous arrival," *Aerospace Science and Technology*, vol. 82-83, pp. 243–251, 2018.

[38] G. Li, Y. Wu, and P. Xu, "Fixed-time cooperative guidance law with input delay for simultaneous arrival," *International Journal of Control*, vol. 94, no. 6, pp. 1664–1673, 2021.

[39] Z. Chen, W. Chen, X. Liu, and J. Cheng, "Three-dimensional fixed-time robust cooperative guidance law for simultaneous attack with impact angle constraint," *Aerospace Science and Technology*, vol. 110, article 106523, 2021.

[40] Y. Wang, Y. Song, D. J. Hill, and M. Krstic, "Prescribed-time consensus and containment control of networked multiagent systems," *IEEE Transactions on Cybernetics*, vol. 49, no. 4, pp. 1138–1147, 2019.

[41] Y. Ren, W. Zhou, Z. Li, Z. Liu, and Y. Sun, "Prescribed-time cluster lag consensus control for second-order non-linear leader-following multiagent systems," *ISA Transactions*, vol. 109, pp. 49–60, 2021.

[42] X. Liao and L. Ji, "On pinning group consensus for dynamical multi-agent networks with general connected topology," *Neurocomputing*, vol. 135, pp. 262–267, 2014.